

Fig. 8. TLR3 signaling by dsRNA contained in apoptotic vesicles induces MoDC maturation. (A) HCV-infected apoptotic Huh7.5.1 cells were labeled with SNARF1. dsRNA was detected in HCV-infected apoptotic cells and vesicles (arrow) by immunofluorescent assay (upper panel) and FACS using anti-dsRNA mAb (lower panel). (B, C) MoDCs were exposed to HCV-infected apoptotic cells for 4 hours and harvested for immunofluorescent assay. The MoDCs were isolated with Ficol-Paque and stained with mAbs against dsRNA or human TLR3. (D) MoDCs were transfected with total RNA extracted from HCV-infected or noninfected Huh7.5.1 cells. After 1 day of culture, the levels of IL-6 were determined. Poly I:C was positive control. (E) The level of TLR3 messenger RNA (mRNA) was determined 1 day after siRNA electroporation. (F) Knockdown of TLR3 partially abolishes the IL-6 production by MoDCs. Data shown are means  $\pm$  SD of duplicate or triplicate samples from one experiment representative of three donors. (G) Poly I:C-transfected apoptotic Huh7.5.1 cells induced MoDCs to produce IL-6.

inflammatory cytokine was a representative marker for TLR3 signal in this case, suggesting that at least HCV RNA, rather than proteins, participates in MoDC maturation.

Since siRNA knockdown of TLR3 in MoDCs was successfully executed by electroporation of MoDCs with TLR3-targeted siRNA (Fig. 8E), we tested whether the level of IL-6 was affected in the TLR3-depleted MoDCs stimulated with apoptotic vesicles containing dsRNA of HCV propagation. TLR3-depleted MoDCs retarded maturation into decreased IL-6 production (Fig. 8F). Poly I:C-transfected Huh7.5.1 apoptotic cells stimulate MoDCs to secrete IL-6 (Fig. 8G). Taken together, phagocytosed HCV-infected apoptotic cells can provoke TLR3 signaling in MoDCs, which participates in MoDC maturation.

MoDCs are known to take up polyI:C, a synthetic dsRNA, which is recognized by TLR3. Therefore, MoDC maturation may be elicited by direct MoDC uptake of dsRNA produced during HCV replication. However, CD86 up-regulation was not observed on MoDCs stimulated with freeze/thaw cell lysates and sonicated apoptotic

cells from HCV-infected Huh7.5.1 cells (Fig. 9A). For MoDC maturation, dsRNA was required to be wrapped in vesicles.

We next treated MoDCs with CPZ (a known inhibitor of clathrin-mediated endocytosis), BAF (a specific inhibitor of the vacuolar H<sup>+</sup>-adenosine triphosphatase), and methyl-beta-cyclodextrin (M $\beta$ CD, which depletes or sequesters membrane cholesterol, inhibiting endocytic pathways dependent on lipid rafts) to evaluate the possible involvement of endocytosis in MoDC maturation. M $\beta$ CD had an inhibitory effect on MoDC maturation (Fig. 9B) and cytokine responses (data not shown) by HCV-infected apoptotic cells. Lipid rafts appeared to play some important roles in the uptake of HCV-infected apoptotic cells.

## Discussion

MoDC recognizes pattern molecules of pathogen to signal the presence of microbial infection.<sup>7</sup> Pattern recog-

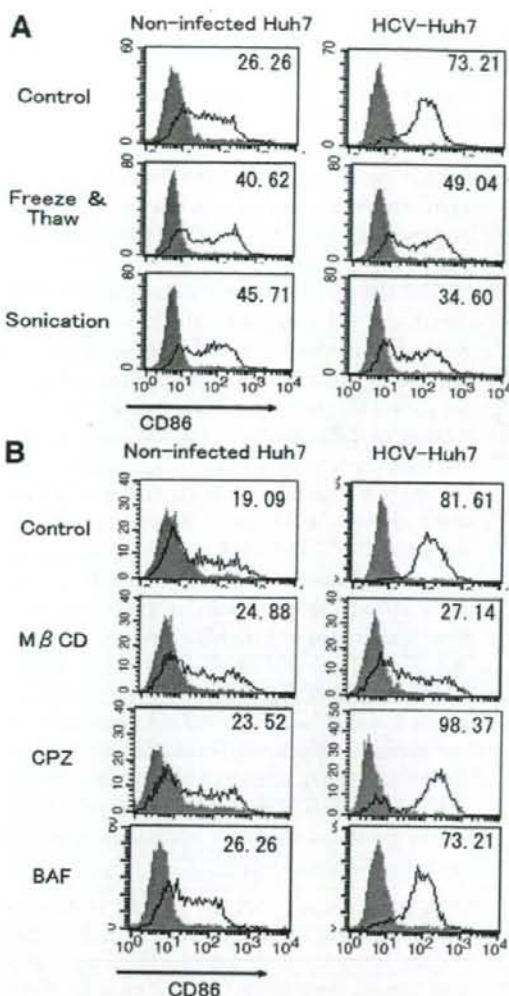


Fig. 9. Lipid raft-dependent phagocytosis of dsRNA-including apoptotic vesicles is required for MoDC maturation. (A) HCV-infected or noninfected apoptotic cells were prepared as described. The expression of CD86 was examined on MoDCs stimulated with apoptotic cell lysates prepared by freeze-thaw or sonication. (B) MoDCs were treated with methyl-beta-cyclodextrin (M $\beta$ CD), CPZ, and BAF for 1 hour, followed by coculture with HCV-infected or noninfected apoptotic cells for 2 days. The MoDC CD86 expression was determined by FACS. Data from a representative of three donors are shown.

nition and antigen uptake are two central events in the activation of cellular immunity. How HCV infection elicits MoDC maturation and NK activation is the theme of this study. The following results were obtained with the JFH1 HCV strain and human MoDC. MoDCs mature via phagocytosing infected hepatocytes, but not through direct infection. MoDCs taking up HCV-infected apo-

ptotic vesicles containing dsRNA activate T cells and NK cells. The mature MoDCs also polarized CD4<sup>+</sup> T cells into the Th1 type. Thus, HCV-infected apoptotic hepatocytes are a source of HCV antigen and PAMPs.

These *in vitro* results cast light on the mechanism of CTL and NK cell activation against HCV in patients. In the liver of patients, immature human MoDCs may phagocytose bystander hepatocytes when the cells undergo apoptosis secondary to HCV infection. The MoDCs that incorporate HCV-infected vesicles into the phagosomes are able to secrete cytokines including IFN- $\beta$  and IL-6. These MoDC responses are enabled by fusing HCV-derived dsRNA with phagosomal TLR3. Activation of the MoDC TLR3 pathway, as has been reported,<sup>8,16</sup> have a crucial role in development of the MoDC TLR3-mediated NK activation and CTL induction.

MoDCs express endogenous DC-SIGN, which captures pseudotype lentivirus particles expressing HCV glycoproteins E1 and E2 and may transmit HCV particles to adjacent hepatocytes.<sup>24</sup> Pseudotype vesicular stomatitis virus coated with chimeric E1 and E2 enters MoDCs through interaction with lectins.<sup>22</sup> These pseudotype HCV studies suggested that MoDCs capture, and in some cases internalize, HCV particles only when expressing E1/E2. In fact, many candidates of the HCV entry receptor have been reported and MoDCs express CD81, scavenger receptor class B type I, and DC-SIGN.<sup>24,25</sup> However, the actual ligand-receptor interaction in HCV-MoDC infection has not been demonstrated even in CD81 and DC-SIGN. Our results suggest that phagocytosis of HCV-infected apoptotic cells, but not direct interaction between MoDCs and HCV particles, serves as an inducer of MoDC maturation. The molecules on HCV-infected cells rather than those only in the virion may participate in induction of MoDC-mediated HCV cellular immunity.

NK cells play a role to prevent persistent HCV infection. An epidemiologic survey showed that genes encoding the weak inhibitory NK cell receptor KIR2DL3 and its human leukocyte antigen C group I ligand are directly associated with HCV eradication in patients.<sup>3</sup> Since the cell-cell contact is indispensable for MoDC-mediated NK activation, soluble factors such as type I IFN and IL-15 may only have a peripheral role in the emergence of HCV-derived NK cells. We have shown that natural killer group 2, member D (NKG2D) ligands on MoDCs, which interact with NKG2D on NK cells are involved in MoDC-mediated NK cell activation against RNA virus infection and poly I:C.<sup>9</sup> The NKG2D/NKG2D ligand interaction was partially responsible for NK activation by MoDCs after uptake of dsRNA-containing vesicles (data

not shown). Yet the main ligand for NK activation on MoDCs is still undetermined. Searching for dsRNA-inducible NK activation ligands in MoDCs would foster identification of MoDC factors reciprocally activating NK cells.

In general, high replication of viruses results in cell death by apoptosis and necrosis. Our study on HCV suggests that apoptotic alteration occurs in HCV-infected Huh7.5.1 cells. These HCV-infected cells fostered MoDCs to produce IL-6 (Fig. 5A) and activate NK cells and T cells regardless of their apoptotic alteration by TNF- $\alpha$  and cycloheximide (data not shown). There is also evidence showing that apoptotic lesions exist in the liver of patients with HCV hepatitis by histological examination.<sup>26</sup> Hence, it is acceptable that MoDCs take up apoptotic hepatocytes that contain HCV antigens and dsRNA in that lesion. Schulz et al.<sup>8</sup> reported that TLR3 in myeloid DCs promotes cross-priming to virus-infected cells using mouse bone marrow-derived DCs and Vero cells containing polyI:C or infected with dsRNA-producing picornavirus.<sup>8</sup> This model study, however, regrettably involves the process of xenogeneic cell-cell interaction. Nevertheless, our present study supports their notion in the human system and offers the possibility that myeloid DC maturation is reproduced by HCV-infected hepatocytes in HCV patients.

There have been many controversial reports about whether MoDCs were infected with HCV and deficient in the allostimulatory capacity in patients with chronic HCV infection.<sup>10</sup> A number of HCV proteins were suggested to affect MoDC function by overexpression studies. HCV core and E1 proteins inhibit the MoDC allostimulatory activity.<sup>27</sup> NS3/4A is a protease that inactivates the IFN-inducing pathways by cleaving the adapter molecules of RIG-I/MDA5 and TLR3, MAVS/Cardif/IPS-1/VISA,<sup>11</sup> and TICAM1/TRIF,<sup>12</sup> respectively. However, these proteins may not be authors for myeloid DC modulation, since HCV replication in MoDCs was not detected *in vitro* and HCV replicates in MoDCs from HCV patients were at very low copy numbers, if any.<sup>10</sup> Although defective MoDCs were reported to appear in HCV patients,<sup>10</sup> this may not merely be due to the DC-HCV interaction since HCV perturbs many cells and mediators in infected lesions.

In the HCV-infected apoptotic cells, there are HCV proteins as well as HCV-derived dsRNA. Therefore, the possibility still remains that not only dsRNA but also phagocytosed HCV proteins are involved in MoDC maturation. Although what happens in HCV natural infection is unclear, our study revealed that MoDC does not mature in response to lysates of HCV-infected apoptotic cells.

Sensor proteins for dsRNA reside in the cytoplasm as well as the cell surface.<sup>7</sup> In MoDCs, MDA5 and RIG-I may be engaged in sensors for HCV dsRNA in HCV-infected apoptotic cells. In this case, however, the dsRNA in phagosomes must pass through the membrane to encounter cytosolic RIG-I/MDA5. Thus, the possible interpretation is that apoptotic vesicles with HCV dsRNA are incorporated into the TLR3-bearing phagosome in MoDCs (Fig. 8C).

TLR3 is the receptor for dsRNA on the endosome membrane and engaged in MoDC maturation.<sup>18</sup> This maturation is inhibited by BAF and chloroquine, indicating that pH changes within intracellular compartments are critical for the process.<sup>28</sup> Opposing to these reports, treating MoDCs with BAF (Fig. 9) or chloroquine (data not shown) results in no inhibition of MoDC maturation in our HCV-incorporated vesicle studies. One possibility deduced from the BAF test is the presence of an alternative source for viral dsRNA recognition that is independent of endosomal acidification. Lipid rafts wherein HCV-infected apoptotic cells are phagocytosed (Fig. 9), may be associated with acidification-free MoDC maturation. Our data, including colocalization of dsRNA with TLR3 and partial blocking TLR3 with siRNA also suggested that TLR3 and HCV dsRNA assemble in the same compartment. Further studies on the dsRNA recognition facility in the phagosomes as well as possible participation of MDA5 and RIG-I in MoDC-NK reciprocal activation will be needed to clarify the mechanism of HCV-mediated MoDC maturation.

**Acknowledgment:** We are grateful to Drs. H. Oshiumi, M. Sasai, A. Ishii, K. Funami, and A. Matsuo in our laboratory for their experimental support. We appreciate Drs. K. Shimotohno (Kyoto University, Kyoto) and Y. Matsuura (Osaka University, Osaka) for their critical discussions. Thanks are also due to Drs. Chisari (The Scripps Research Institute, La Jolla, CA) for providing the cell line.

## References

1. Poynard T, Yuen MF, Ratziu V, Lai CL. Viral hepatitis C. *Lancet* 2003; 362:2095-2100.
2. Haller O, Kochs G, Weber F. The interferon response circuit: induction and suppression by pathogenic viruses. *Virology* 2006;344:119-130.
3. Khakoo SI, Thio CL, Martin MP, Brooks CR, Gao X, Astemborski J, et al. HLA and NK cell inhibitory receptor genes in resolving hepatitis C virus infection. *Science* 2004;305:872-874.
4. Chang KM, Thimme R, Melpolder JJ, Oldach D, Pemberton J, Moorhead-Loudis J, et al. Differential CD4(+) and CD8(+) T-cell responsiveness in hepatitis C virus infection. *HEPATOLOGY* 2001;33:267-276.
5. Thimme R, Oldach D, Chang KM, Steiger C, Ray SC, Chisari FV. Determinants of viral clearance and persistence during acute hepatitis C virus infection. *J Exp Med* 2001;194:1395-1406.

6. Bigger CB, Brasky KM, Lanford RE. DNA microarray analysis of chimpanzee liver during acute resolving hepatitis C virus infection. *J Virol* 2001;75:7059-7066.
7. Akira S, Uematsu S, Takeuchi O. Pathogen recognition and innate immunity. *Cell* 2006;124:783-801.
8. Schulz O, Diebold SS, Chen M, Naslund TI, Nolte MA, Alexopoulou L, et al. Toll-like receptor 3 promotes cross-priming to virus-infected cells. *Nature* 2005;433:887-892.
9. Andrews DM, Andoniou CE, Scalzo AA, van Dommelen SL, Wallace ME, Smyth MJ, et al. Cross-talk between dendritic cells and natural killer cells in viral infection. *Mol Immunol* 2005;42:547-555.
10. Pachiadakis I, Pollara G, Chain BM, Naoumov NV. Is hepatitis C virus infection of dendritic cells a mechanism facilitating viral persistence? *Lancet Infect Dis* 2005;5:296-304.
11. Li XD, Sun L, Seth RB, Pineda G, Chen ZJ. Hepatitis C virus protease NS3/4A cleaves mitochondrial antiviral signaling protein off the mitochondria to evade innate immunity. *Proc Natl Acad Sci U S A* 2005;102:17717-17722.
12. Li K, Foy E, Ferreon JC, Nakamura M, Ferreon AC, Ikeda M, et al. Immune evasion by hepatitis C virus NS3/4A protease-mediated cleavage of the Toll-like receptor 3 adaptor protein TRIF. *Proc Natl Acad Sci U S A* 2005;102:2992-2997.
13. Wakita T, Pietschmann T, Kato T, Date T, Miyamoto M, Zhao Z. Production of infectious hepatitis C virus in tissue culture from a cloned viral genome. *Nat Med* 2005;11:791-796.
14. Zhong J, Gastaminza P, Cheng G, Kapadia S, Kato T, Burton DR, et al. Robust hepatitis C virus infection in vitro. *Proc Natl Acad Sci U S A* 2005;102:9294-9299.
15. Lee HK, Lund JM, Ramanathan B, Mizushima N, Iwasaki A. Autophagy-dependent viral recognition by plasmacytoid dendritic cells. *Science* 2007;315:1398-1401.
16. Akazawa T, Ebihara T, Okuno M, Okuda Y, Shingai M, Tsujimura K, et al. Antitumor NK activation induced by the Toll-like receptor 3-TI-CAM-1 (TRIF) pathway in myeloid dendritic cells. *Proc Natl Acad Sci U S A* 2007;104:252-257.
17. Ebihara T, Masuda H, Akazawa T, Shingai M, Kikuta H, Ariga T, et al. NKG2D ligands are induced on human dendritic cells by TLR ligand stimulation and RNA virus infection. *Int Immunol* 2007;19:1145-1155.
18. Matsumoto M, Funami K, Tanabe M, Oshiumi H, Shingai M, Seto Y, et al. Subcellular localization of Toll-like receptor 3 in human dendritic cells. *J Immunol* 2003;171:3154-3162.
19. Castet V, Fournier C, Soulier A, Brillet R, Coste J, Larrey D, et al. Alpha interferon inhibits hepatitis C virus replication in primary human hepatocytes infected in vitro. *J Virol* 2002;76:8189-8199.
20. Sosnovtsev SV, Prikhod'ko EA, Belliot G, Cohen JJ, Green KY. Feline calicivirus replication induces apoptosis in cultured cells. *Virus Res* 2003;94:1-10.
21. Prechtel AT, Turza NM, Theodoridis AA, Steinkasserer A. CD83 knockdown in monocyte-derived dendritic cells by small interfering RNA leads to a diminished T cell stimulation. *J Immunol* 2007;178:5454-5464.
22. Kaimori A, Kanto T, Kwang C, Limn, Komoda Y, Oki C, et al. Pseudotype hepatitis C virus enters immature myeloid dendritic cells through the interaction with lectin. *Virology* 2004;324:74-83.
23. Heil F, Hemmi H, Hochrein H, Ampenberger F, Kirschning C, Akira S, et al. Species-specific recognition of single-stranded RNA via toll-like receptor 7 and 8. *Science* 2004;303:1526-1529.
24. Cormier EG, Durso RJ, Tsarnis F, Boussemart L, Manix C, Olson WC, et al. L-SIGN (CD209L) and DC-SIGN (CD209) mediate transinfection of liver cells by hepatitis C virus. *Proc Natl Acad Sci U S A* 2004;101:14067-14072.
25. Yamada E, Montoya M, Schuetzler CG, Hickling TP, Tarr AW, Vitelli A, et al. Analysis of the binding of hepatitis C virus genotype 1a and 1b E2 glycoproteins to peripheral blood mononuclear cell subsets. *J Gen Virol* 2005;86:2507-2512.
26. Kountouras J, Zavos C, Chatzopoulos D. Apoptosis in hepatitis C. *J Viral Hepat* 2003;10:335-342.
27. Sarobe P, Lasarte JJ, Zabaleta A, Arribillaga L, Arina A, Melero I, et al. HCV structural proteins impair dendritic cell maturation and inhibit in vivo induction of cellular immune responses. *J Virol* 2003;77:10862-10871.
28. de Bouteiller O, Merck E, Hasan UA, Hubac S, Benguigui B, Trinchieri G, et al. Recognition of double-stranded RNA by human toll-like receptor 3 and downstream receptor signaling requires multimerization and an acidic pH. *J Biol Chem* 2005;280:38133-38145. 6.

# Human T<sub>H</sub>1 differentiation induced by lipoarabinomannan/lipomannan from *Mycobacterium bovis* BCG Tokyo-172

Toshihiro Ito<sup>1</sup>, Akihiro Hasegawa<sup>1</sup>, Hiroyuki Hosokawa<sup>1</sup>, Masakatsu Yamashita<sup>1</sup>, Shinichiro Motohashi<sup>1</sup>, Takashi Naka<sup>2</sup>, Yuko Okamoto<sup>2</sup>, Yukiko Fujita<sup>2</sup>, Yasuyuki Ishii<sup>3</sup>, Masaru Taniguchi<sup>3</sup>, Ikuya Yano<sup>2</sup>, and Toshinori Nakayama<sup>1</sup>

<sup>1</sup>Department of Immunology, Graduate School of Medicine, Chiba University, 1-8-1 Inohana, Chuo-ku, Chiba 260-8670, Japan

<sup>2</sup>Japan BCG Laboratory, 3-1-5 Matsuyama, Kiyose, Tokyo 204-0022, Japan

<sup>3</sup>RIKEN Research Center for Allergy and Immunology, 1-7-22 Suehiro-cho, Tsurumi-ku, Yokohama, Kanagawa 230-0045, Japan

Keywords: DC, T<sub>H</sub>1/T<sub>H</sub>2, vaccination

## Abstract

*Mycobacterium tuberculosis* (tubercle bacilli) and the related acid-fast bacteria including *Mycobacterium bovis* Bacille Calmett–Guerin (BCG) have a characteristic cell wall (CW) containing various lipoglycans and glycolipids. Such lipoglycans have been reported to activate type-1 inflammatory responses via dendritic cells (DCs) through Toll-like receptor 2. In this study, lipoglycans, lipoarabinomannan (LAM), lipomannan (LM) and phosphatidylinositol mannoside (PIM), were purified from the CW fractions of *M. bovis* BCG Tokyo-172, and the effect on the differentiation of human peripheral blood naive CD4 T cells into T<sub>H</sub>1 and T<sub>H</sub>2 was examined. LAM/LM molecules enhanced T<sub>H</sub>1 differentiation under both T<sub>H</sub>1 and T<sub>H</sub>2 conditions, whereas some other glycolipids and phospholipid enhanced T<sub>H</sub>2 differentiation under T<sub>H</sub>2 conditions. Other components had little effect under the given conditions. Even in highly purified CD4 T cell cultures, LAM/LM enhanced T<sub>H</sub>1 generation only under T<sub>H</sub>1 culture conditions. These results indicate that LAM/LM possesses a potent augmenting activity in T<sub>H</sub>1 differentiation in human CD4 T cells. LAM/LM appeared to act directly on naive CD4 T cells to enhance T<sub>H</sub>1 differentiation under T<sub>H</sub>1 culture conditions, while acting indirectly to up-regulate the generation of T<sub>H</sub>1 cells via IL-12/DCs under T<sub>H</sub>1 and T<sub>H</sub>2 conditions. Therefore, these results provide the first evidence indicating that LAM/LM from *M. bovis* BCG may possess a potent modulating activity in the human system, and thus supporting the strategy for the use of BCG components in the vaccine development for such T<sub>H</sub>2 diseases as allergic asthma and rhinitis.

## Introduction

The mycobacterial cell envelope consists of diverse lipophilic components such as mycoloyl glycolipids, lipomannan (LM)/lipoarabinomannans (LAM), lipopeptides and phosphatidylinositol mannosides (PIMs) or cardiolipin as shown schematically in Fig. 1 (1, 2). LAM is a major amphipathic molecule in the cell wall (CW) components of mycobacteria and is regarded as a modulin acting through its diverse immunoregulatory and anti-inflammatory effects, which may support the survival of the mycobacteria within the infected hosts. These effects are mediated by the inhibition of IFN- $\gamma$ -dependent activation of macrophages (3, 4), inhibition of antigen-induced T cell proliferation (5) and scavenging of oxygen-derived free radicals (6). LAM acts as a virulence factor responsible for macrophage deactivation by

mannose receptor down-regulation and also is implicated in phagocytosis of mycobacteria (7). Furthermore, PIMs, that are assumed to be precursors of LM and LAM have recently been proposed to recruit NKT cells, which play a primary role in the granulomatous response in mycobacterial infection (8, 9). The precursor–product relationship of phosphatidylinositol (PI), PIMs, LM and LAM has recently been proposed based on biosynthetic (1, 10) and genetic studies (11, 12), but the details of this pathway remain unclear. On the other hand, however, the structures of LAM from many species of mycobacteria, nocardia and rhodococcus including *Mycobacterium tuberculosis*, *Mycobacterium leprae*, *M. bovis* Bacille Calmett–Guerin (BCG) and *Mycobacterium smegmatis* have been vigorously investigated over the last

Correspondence to: T. Nakayama; E-mail: tnakayama@faculty.chiba-u.jp

Transmitting editor: A. Singer

Received 8 November 2007, accepted 8 April 2008

Advance Access publication 9 May 2008

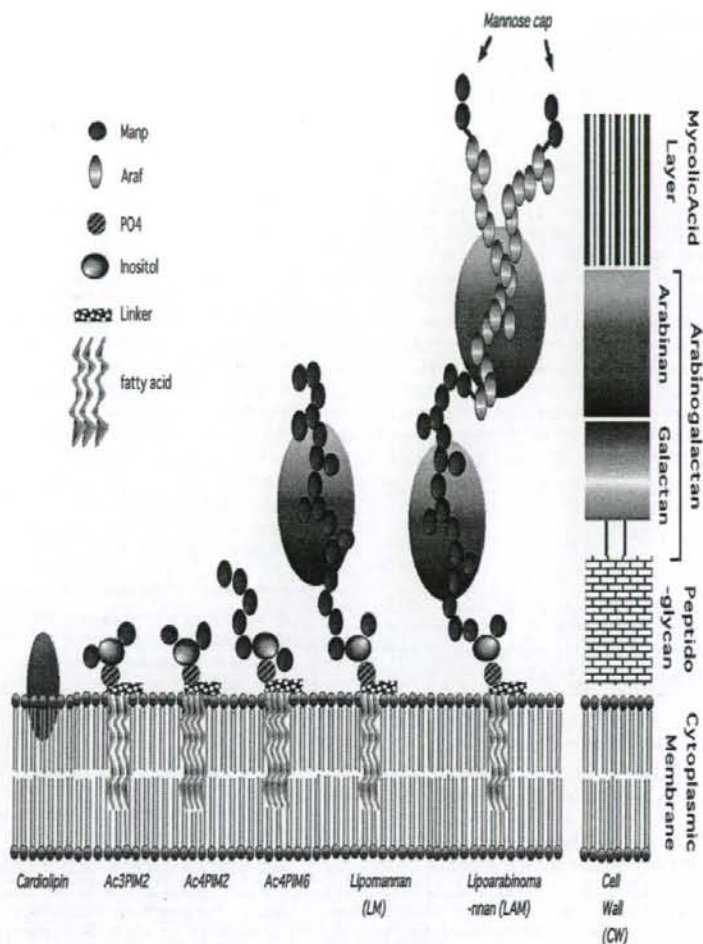


**Fig. 1.** Schematic structure of the mycobacterial cell envelopes. The individual compartment was shown to be a cytoplasmic membrane, peptidoglycan layer, arabinogalactan and mycolic acid layer (right side). The structures of the major lipid and lipoglycan molecules from BCG Tokyo-172 are shown; cardiolipin, Ac3PIM2, Ac4PIM2, Ac4PIM6, LM and LAM.

decade. LAM is a complex lipoglycan composed of D-mannan and D-arabinan attached to a PI moiety that anchors to the cytoplasmic membrane in the mycobacterial cell envelope (13). Although fatty acyl moiety is consistent among mycobacteria, the carbohydrate chain structure of LAM differs greatly according to the mycobacterial species, such as LAM with mannose caps (ManLAM), AraLAM and PILAM. However, the relationship between the molecular structure and immunomodulating activity of LAM has not yet been fully established especially in human immunocompetent systems.

Dendritic cells (DCs) play a crucial role in the induction of cellular immunity against intracellular pathogens including mycobacteria (14–16). Human or murine myeloid DC infected with *M. tuberculosis* or *M. bovis* BCG induced the

maturation with an increased IL-12 production (17, 18) and induced a potent anti-tuberculous immunity against experimental tuberculosis in mice (19). A  $T_H1$  cytokine IFN- $\gamma$  has been identified as a key cytokine controlling mycobacterial infections (20–23). Patients defective in genes for IFN- $\gamma$  or the IFN- $\gamma$ R are prone to serious mycobacterial infections (24). Therefore, IFN- $\gamma$  plays a crucial role in anti-mycobacterial immunity. ManLAM, which is produced by slow-growing mycobacteria including *M. bovis* BCG, which has been reported to exert an immunosuppressive effect (25–27) and contributes to the persistence of slow-growing mycobacteria in humans. In contrast, LAM having phospho-myo-inositol units and LAM without capping are called PILAM and are produced from fast-growing mycobacteria. PILAM produces

a variety of pro-inflammatory cytokines through the activation of Toll-like receptor 2 (TLR2) (28–30). LM was shown to activate the macrophages in a TLR2-dependent and TLR4- and TLR6-independent manner (31–33). The balance of ManLAM/LM could thus be a parameter influencing the net immune responses against mycobacteria (34). Many investigators have reported that LAM/LM molecules induced type-I inflammatory cytokines, such as tumor necrosis factor  $\alpha$  (TNF $\alpha$ ) and IL-12 in DCs, and increased CD1 molecules on antigen-presenting cells (APCs). However, the regulation of the  $T_H1/T_H2$  balance in the human immune system with PBMC induced by LAM/LM has not yet been reported.

In the present study, purified ManLAM/LM molecules from *M. bovis* BCG Tokyo-172 were structurally and functionally characterized, and the effect of LAM/LM on  $T_H1/T_H2$  differentiation was assessed using an established human  $T_H1/T_H2$  differentiation culture system. As a result, two distinct regulatory pathways were identified in which mycobacterial LAM/LM controls the balance of  $T_H1/T_H2$  directly or indirectly via APCs.

## Methods

### Bacterial strain and growth conditions

*Mycobacterium bovis* BCG Tokyo-172 (ATCC 35737) was grown as a surface culture at 37°C in Sauton medium for 8 days. The bacterial culture was harvested by centrifugation after autoclaving at 121°C for 15 min.

### Isolation and purification of LAM/LM, phosphatidylinositol dimannoside, hexamannoside and cardiolipin

Lipids were extracted with chloroform-methanol (2:1, by volume) and the crude lipids were separated by the solvent fractionation method (35). The PIMs [phosphatidylinositol dimannoside (PIM2) and hexamannoside (PIM6)] and cardiolipin were isolated from the chloroform-soluble fraction by thin-layer chromatography on a silica gel (Uniplate and Analtech) with the solvent system of chloroform-methanol-water (65:25:4, by volume). For purification of LAM/LM, the cells were re-suspended in deionized water and were passed three times through a French pressure cell (5501-MF, OHTAKE WORKS, Tokyo, Japan) at a pressure of 180 Mpa and disrupted. The unbroken cells were removed by centrifugation twice at  $6760 \times g$  for 20 min at 25°C. The broken cells (crude CW fraction) were separated from the supernatant by ultracentrifugation at  $18\,000 \times g$  for 1 h at 25°C, and the supernatant containing lipoglycan was lyophilized. Contaminating glucans, proteins, DNA and RNA were removed by enzymatic degradation using  $\alpha$ -amylase, trypsin, DNase 1 and RNase treatments followed by dialysis. An equal volume of 90% phenol was then added to the water containing lipoglycans, and the mixture was incubated with shaking at 68°C for 1 h. After separation of the aqueous phase from the phenol layer by low-speed centrifugation, the phenolic phase was again extracted with an equal volume of water. The two aqueous extracts were combined and residual phenol was removed by extraction with the chloroform. The aqueous phase containing the crude lipogly-

cans was evaporated to dryness. The crude lipoglycans were subjected to Triton X-114 phase separation (36). The resulting lipoglycans (LAM/LM) were re-suspended in buffer A, 0.2 M NaCl, 0.25% sodium deoxycholate (w/v), 1 mM EDTA and 10 mM Tris, pH 8.0, and loaded onto gel filtration columns (Superdex 75 prep grade column,  $50 \times 1$  cm, Amersham Bioscience) and eluted with buffer A at a flow rate  $0.2 \text{ ml min}^{-1}$ . The fractions were collected and analyzed by SDS-PAGE followed by silver staining. The LAM and LM fractions pooled were dialyzed extensively against water, lyophilized and stored at  $-20^\circ\text{C}$ .

### Mass spectrometric analysis of lipoglycans LAM and LM

MALDI TOF-MS spectra were acquired on a Voyager DE-STR MALDI TOF-MS spectrometer (Applied Biosystem) with a pulse laser emitting at 337 nm. The samples were analyzed in the reflectron mode with an accelerating voltage operating in the negative ion mode of 25 kV. As the matrix, 2,5-dihydroxybenzoic acid was used at a concentration of  $10 \text{ mg ml}^{-1}$ , in a mixture of water. A total of  $1.0 \mu\text{l}$  of lipoglycan, at a concentration of  $10 \text{ mg ml}^{-1}$ , was mixed with  $1.0 \mu\text{l}$  of the matrix solution. The sample mixture was applied onto the sample plate as a  $1.0\text{-}\mu\text{l}$  droplet. The samples were then allowed to crystallize at room temperature.

### Preparation of human PBMCs and CD4 T cells

Whole blood was obtained from six healthy donor volunteers between 24 and 50 years old. The protocol was approved by the Institutional Ethics Committee (No. 1972). PBMCs were isolated by Ficol-Paque (Pharmacia-Upjohn, Uppsala, Sweden) gradient centrifugation (37). Naive CD4 $^+$  T cells were stained with anti-CD8/CD45RO-FITC and then purified using anti-FITC magnetic beads (Milteny Biotec) and AutoMACS cell sorter (Milteny Biotec) by negative sorting.

### Preparation of highly purified naive CD4 T cells and monocyte derived dendritic cells

Highly purified naive CD4 T cells (CD4 $^+$ , CD45RA $^+$ ) were prepared using a human naive CD4 T cell isolation kit (Milteny Biotec Inc.) and an AutoMACS sorter. The purity (CD4 $^+$ , CD45RA $^+$ ) was >95%. For preparation of monocyte derived dendritic cells, whole PBMCs were allowed to adhere to culture flasks for 1.5–2 h at 37°C and then adherent cells were cultured for 5–7 days in the presence of human IL-4 ( $500 \text{ U ml}^{-1}$ , R&D Systems, Minneapolis, MN, USA) and human granulocyte macrophage colony-stimulating factor ( $800 \text{ U ml}^{-1}$ ) (38). CD11c $^+$  cells were purified using a MACS separation column (Milteny Biotec) according to the manufacturer's protocol. Purified DCs ( $7.5 \times 10^5$  per well) were added to the *in vitro* T cell differentiation culture.

### In vitro T cell differentiation culture

Naive CD4 T cells or highly purified naive CD4 T cells ( $7.5 \times 10^5$  per well) were stimulated with  $20 \mu\text{g ml}^{-1}$  immobilized anti-CD3 mAb (Raritan, Somerset County, NJ, USA) for 2 days in the presence of  $50 \text{ U ml}^{-1}$  IL-2 (Shionogi & Co., Ltd, Osaka, Japan),  $1 \text{ ng ml}^{-1}$  IL-12 (R&D Systems) and  $5 \mu\text{g ml}^{-1}$  anti-IL-4 mAb (BD Bioscience) under  $T_H1$  culture conditions (39). For  $T_H2$  conditions, the cells were stimulated with  $20 \mu\text{g ml}^{-1}$  immobilized anti-CD3 mAb in the presence of

852 Human  $T_H1$  generation by ManLAM/LM in *M. bovis* BCG

50 U ml<sup>-1</sup> IL-2, 1 ng ml<sup>-1</sup> IL-4 (R&D Systems) and 5 µg ml<sup>-1</sup> anti-IFN-γ mAb (BD Bioscience). For neutral conditions, the cells were stimulated with 20 µg ml<sup>-1</sup> immobilized anti-CD3 mAb in the presence of 50 U ml<sup>-1</sup> IL-2. The cells were then transferred to new plates and cultured for another 5 days in the presence of cytokines and antibodies used in the same culture conditions. Since IL-4-producing cells were not induced significantly in a week culture under  $T_H2$  culture conditions, two cycles of the stimulation were used. Where indicated, anti-IL-12 mAb (2 µg ml<sup>-1</sup>, U-CyTech Biosciences, Utrecht, The Netherlands) was added to the culture. The final concentration of CW, LAM/LM, PIM2 and PIM6 was adjusted to 100 µg ml<sup>-1</sup>.

Intracellular staining of IL-4 and IFN-γ and flow cytometry analysis

The cultured T cells were re-stimulated with PMA (10 ng ml<sup>-1</sup>) and ionomycin (1 µM) for 4 h in the presence of 2 µM monensin, which inhibited the secretion of newly produced protein. Next, the cells were fixed with 4% PFA for 10 min at room temperature and were permeabilized with 0.5% Triton X-100 (in 50 mM NaCl, 5 mM EDTA and 0.02% Na<sub>3</sub>PH<sub>7.5</sub>) for 10 min on ice. After blocking with 3% BSA in PBS for 15 min, the cells were incubated on ice for 45 min with anti-IFN-γ-FITC, IL-4-PE (BD Bioscience) and CD4-allophycocyanin (BD Bioscience) as described (39). A flow cytometry

analysis was performed on FACScalibur® (Becton Dickinson, Franklin Lakes, NJ, USA), and the results were analyzed using the CELLQUEST® software program (Becton Dickinson).

Results

Purification of LAM/LM from BCG Tokyo-172

The experimental procedures to extract LM and LAM from *M. bovis* BCG Tokyo-172 are based on successive detergent and phenolic extractions, thus leading to the recovery of nucleic acid-, protein- and lipid-free materials.

LAM and LM fractions were fully separated and collected by gel filtration chromatography (Fig. 2A). The purity of each component was assessed by SDS-PAGE (Fig. 2B), and the molar ratios of mannose and arabinose in LAM and LM fractions were analyzed by gas chromatography/mass spectrometry (data not shown) and MALDI TOF-MS spectrometry (Fig. 2C and D). The accurate molecular weights of LAM and LM were determined on the basis of the deprotonated ions [M-H]<sup>-</sup>. As a result, LAMs from *M. bovis* BCG TOKYO-172 was identified to be highly heterogeneous lipoglycans possessing 16–46 mannose residues and 50–60 arabinoses and three acyl groups with the molecular weight ranging from 11 000 to 19 000 Da (Fig. 2C). On the other hand, LM from *M. bovis* BCG Tokyo-172 showed clear [M-H]<sup>-</sup> ions in MALDI TOF-MS analysis ranging from m/z 3600 to 8400,

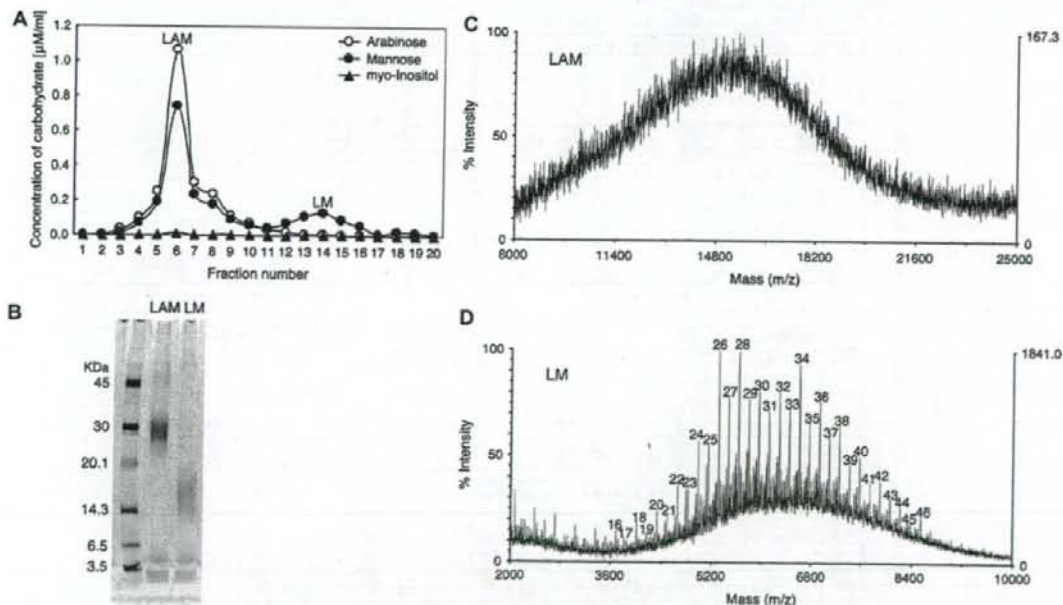


Fig. 2. Purification of BCG Tokyo-172 LAM and LM and MALDI TOF-MS spectra of the purified fractions. (A) Gel filtration profile of the Triton X-114 fraction containing lipoglycans. The fraction was loaded onto a Superdex 75 prep grade column and eluted with deoxycholate buffer. (B) SDS-PAGE analysis of purified fractions from LAM and LM. (C) Negative ion mode MALDI TOF-MS spectra of the fraction LAM. (D) Negative ion mode MALDI TOF-MS spectra of the fraction LM that corresponded to triacylated forms, with 2C16 and 1C19 fatty acids. The numbers shown in the figure represent the number of mannose residues in LM.



indicating that they have 16–48 mannoses and three acyl groups, C16:0, C16:0 and C19:0, mainly (Fig. 2D).

#### Effects of LAM/LM in human $T_H1/T_H2$ cell differentiation

An *in vitro*  $T_H1/T_H2$  differentiation culture system was used with human peripheral blood naive CD4 T cells to evaluate the effects of BCG CW components on human  $T_H1/T_H2$  differentiation. First, the effect of whole CW fraction and the mixture of LAM/LM were assessed. BCG CW components were homogeneously suspended in PBS and then the vehicle was used as negative control. Under  $T_H1$  culture conditions, the generation of  $T_H1$  cells (IFN- $\gamma$  positive and IL-4 negative) was significantly enhanced in the presence of CW and LAM/LM (37.5 versus 80.7 and 73.6%, respectively) in comparison to the vehicle control (Fig. 3A). Under  $T_H2$  culture conditions, the generation of  $T_H2$  (IL-4 positive and IFN- $\gamma$  negative) was inhibited significantly in the presence of CW and LAM/LM (25.7 versus 12.5 and 13.9%, respectively), whereas that of  $T_H1$  was enhanced greatly (10.9 versus 37.6 and 38.8%, respectively). Under neutral conditions, they were cultured for 1 week (Fig. 3A) or 2 weeks (Fig. 3B) with anti-CD3 mAb with IL-2, and the generation of IFN- $\gamma$ -producing  $T_H1$  and that of IL-4-producing  $T_H2$  were marginal, and the levels of these  $T_H1/T_H2$  were not affected in the presence of CW or LAM/LN. These results indicate that CW and LAM/LM enhance  $T_H1$  differentiation and inhibit  $T_H2$  differentiation

under both  $T_H1$  and  $T_H2$  culture conditions. Ac4PIM2, Ac3PIM2, Ac4PIM6 and cardiolipin, which are precursors of LAM/LM and cytoplasmic membrane lipids, did not enhance  $T_H1$  differentiation significantly, but showed some induction of  $T_H2$  under  $T_H2$  culture conditions (Fig. 3C), indicating that the precursors of LAM/LM may have different effects from LAM/LM on  $T_H1/T_H2$  differentiation in human PBMC cultures *in vitro* under the given conditions.

Next, to confirm the effects of CW and LAM/LM on  $T_H1/T_H2$  differentiation, the analysis was extended to naive CD4 T cells from 10 healthy volunteers. Similar  $T_H1/T_H2$  cultures were used in the presence of CW and LAM/LM (Fig. 4). As expected, the addition of CW and LAM/LM to the induction culture enhanced  $T_H1$  differentiation under both  $T_H1$  (Fig. 4A and C) and  $T_H2$  culture conditions (Fig. 4B and D, right panels), and the addition of CW suppressed  $T_H2$  differentiation under  $T_H2$  culture conditions (Fig. 4B, left panel) in most of the healthy volunteers tested. The addition of LAM/LM inhibited  $T_H2$  differentiation in some but not all individuals (Fig. 4D, left panel). Thus, these results clearly indicate that CW and LAM/LM enhance  $T_H1$  differentiation while they inhibit  $T_H2$  differentiation. No significant effect was observed under neutral conditions (Supplementary Figure 1, available at *International Immunology* Online). Ac4PIM2, Ac3PIM2, Ac4PIM6 and cardiolipin did not affect the levels of either  $T_H1$  differentiation under both  $T_H1$  and  $T_H2$  culture conditions

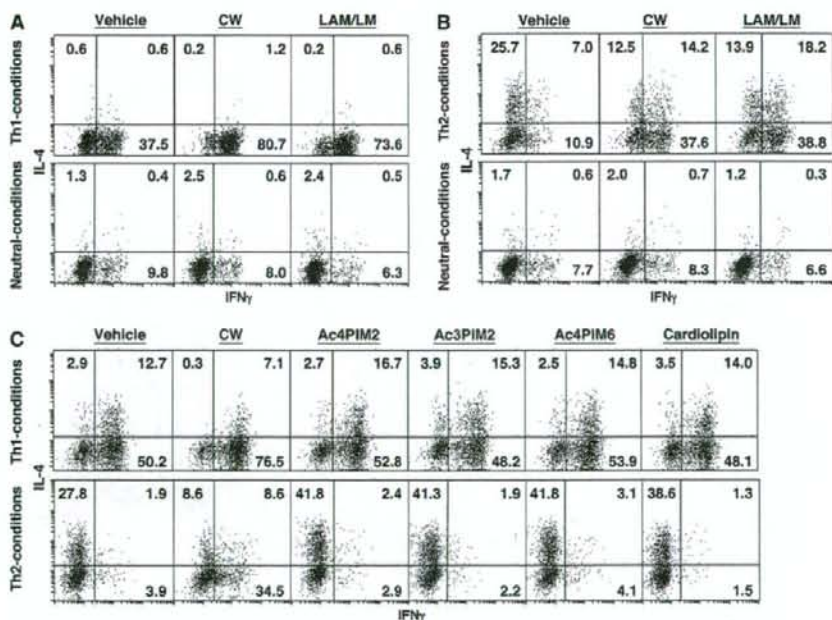


**Fig. 3.** Effect of BCG CW components on human  $T_H1/T_H2$  differentiation. Naive CD4 T cells from human PBMC were stimulated with anti-CD3 ( $20 \mu\text{g ml}^{-1}$ ) in the presence of anti-IFN- $\gamma$  mAb, IL-4 and IL-2 ( $T_H1$  conditions) or in the presence of IL-2 (neutral conditions). The cultured cells were subjected to intracellular staining with anti-IL-4 and anti-IFN- $\gamma$ . A 1-week culture (A) and a 2-week culture (B) were performed. CW and LAM/LM ( $100 \mu\text{g ml}^{-1}$ ) (A and B) or Ac4PIM2, Ac3PIM2, Ac4PIM6 or cardiolipin (C) ( $100 \mu\text{g ml}^{-1}$ ) were added to the culture.

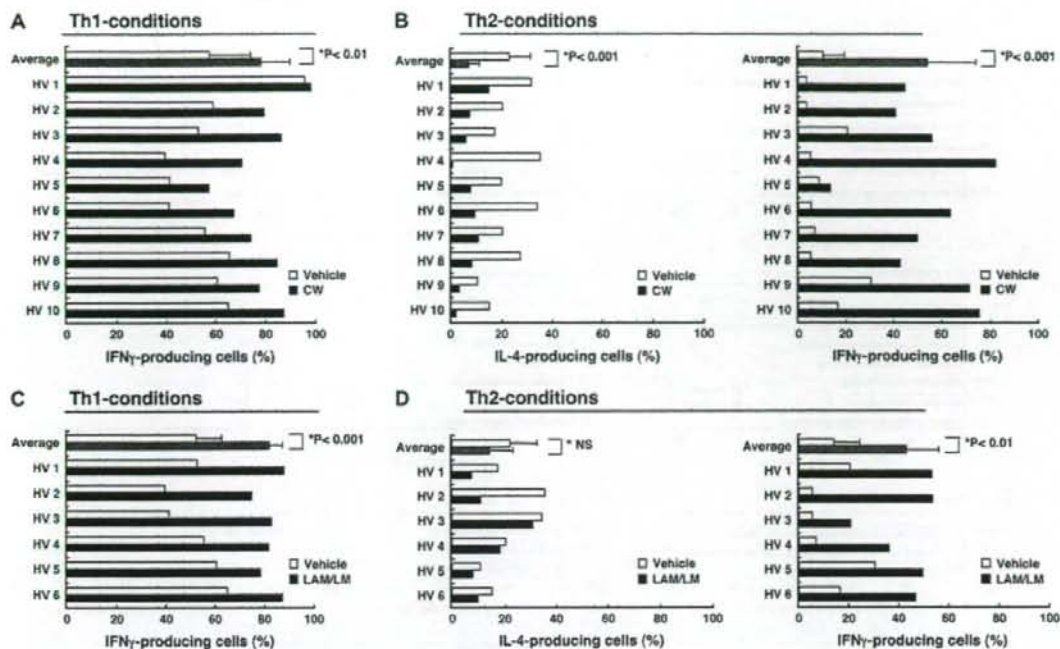


Fig. 4. Effect of BCG CW and LAM/LM on  $T_H1/T_H2$  differentiation using ten human healthy donor PBMCs.  $T_H1/T_H2$  cell differentiation cultures with naive CD4 T cells from 10 human PBMCs were performed as described in Fig. 3. CW (A and B) and LAM/LM (C and D) ( $100 \mu\text{g ml}^{-1}$ ) were added. The mean values with standard deviations are also shown. Statistical analysis was done using Student's *t*-test.

(Fig. 5A–H). In addition, the effect of these components on the differentiation of  $T_H2$  was seen in some cultures but the effects were marginal (Fig. 5B, D, F and H).

*Cellular mechanisms underlying the LAM/LM-mediated modulation of human  $T_H1/T_H2$  differentiation*

The CD4 T cells from human PBMC, which were used in the experiments described above, were prepared by removing CD8<sup>+</sup>CD45RO<sup>+</sup> cells with an AutoMACS cell sorter as described in Methods. These cell preparations contain substantial numbers of forward-scatter<sup>high</sup>/side-scatter<sup>high</sup> cells and CD4-negative cells (Fig. 6A, Fraction A). To further enrich CD4 T cells, a naive CD4 T cell isolation kit and AutoMACS cell sorter were used (Fig. 6B, Fr. B). Positive cells for CD8, CD14, CD16, CD19, CD36, CD45RO, CD56, CD123, TCR $\gamma\delta$  or glycoporin were removed in this separation procedure. Concurrently, CD11c-positive *in vitro* generated DCs from PBMCs were isolated using PE-conjugated anti-CD11c mAb, anti-PE magnetic beads and AutoMACS (Fig. 6C, Fr. C). Using these crude naive CD4 T cells (Fr. A), highly purified naive CD4 T cells (Fr. B) and the mixture of purified naive CD4 T cells (Fr. B) and enriched DCs (Fr. C),  $T_H1/T_H2$  differentiation cultures were set in the presence of LAM/LM (Fig. 7). Under  $T_H1$  culture conditions, the generation of IFN- $\gamma$ -producing cells was enhanced by LAM/LM in all cultures with Fr. A, Fr. B and the mixture of Fr.

B and Fr. C (Fig. 7A, left). Under neutral conditions, the induction of IFN- $\gamma$ -producing cells was marginal after a 1-week culture with Fr. A and Fr. B, and no significant effect was observed (Fig. 7A, right). However, in the culture of the mixture of purified naive CD4 T cells (Fr. B) and DCs (Fr. C), the generation of IFN- $\gamma$ -producing cells was enhanced. Under  $T_H2$  culture conditions, the enhancement of the generation of IFN- $\gamma$ -producing cells and the inhibition of the generation of IL-4-producing cells in the presence of LAM/LM were observed in the cultures with Fr. A but not in the cultures with Fr. B (Fig. 7B, left panels). Interestingly, however, the effects of LAM/LM were restored by the addition of DCs (Fr. C) into purified naive CD4 T cells (Fr. B) (Fig. 7B, left bottom). The addition of anti-IL-12 mAb inhibited the enhancement of the generation of IFN- $\gamma$ -producing cells (10.3 versus 3.2%) and the suppression of the generation of IL-4-producing cells (24.4 versus 40.3%) in the Fr. A cultures. No effect was observed in the Fr. B cultures (15.8 versus 15.4%). A small but moderate rescue effect was observed in the culture with the mixture of Fr. B and Fr. C (3.1 versus 4.5%). Basically, the same pattern as that seen after the 1-week culture (Fig. 7A, right) was observed after the 2-week culture under neutral conditions (Fig. 7B, right). These results indicate that LAM/LM acts directly to CD4 T cells to enhance the generation of IFN- $\gamma$ -producing cells under  $T_H1$  culture conditions and that LAM/LM acts indirectly via DCs

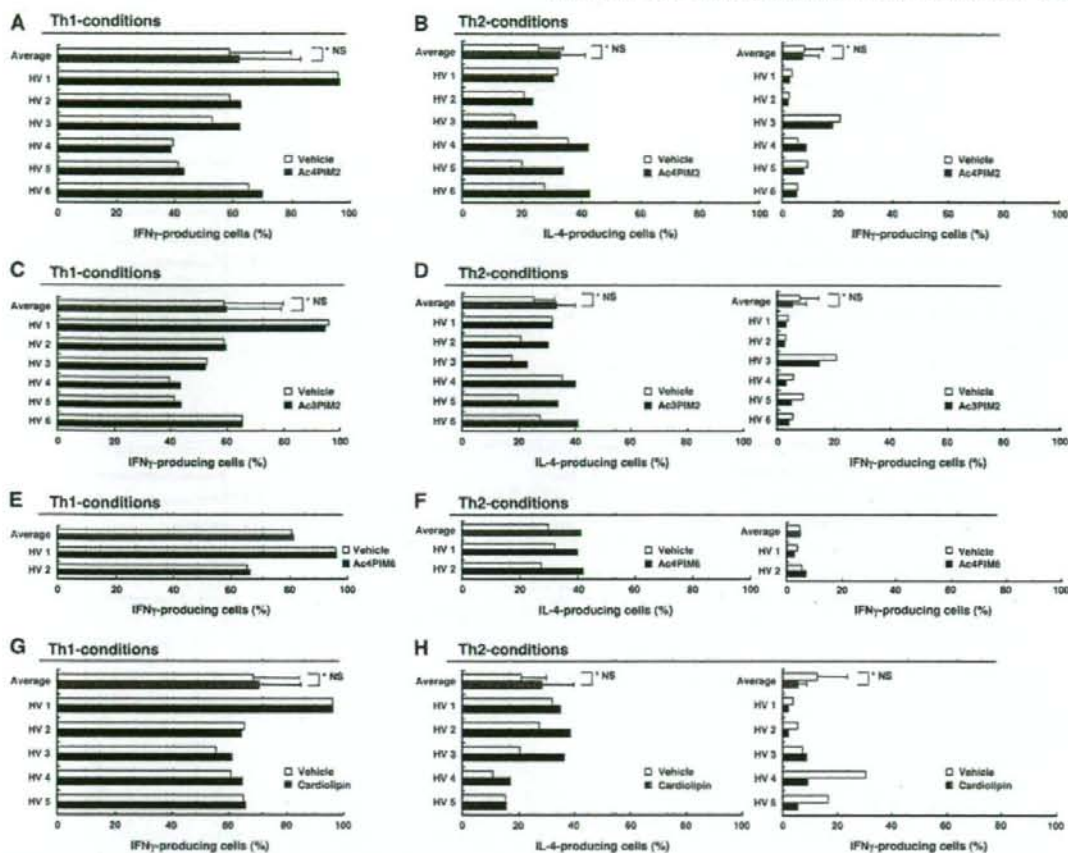


**Fig. 5.** Effect of Ac4PIM2, Ac3PIM2, Ac4PIM6 and cardioliplin on human  $T_H1/T_H2$  differentiation. Effects of Ac4PIM2 under  $T_H1$  (A) or  $T_H2$  (B) conditions, Ac3PIM2 under  $T_H1$  (C) or  $T_H2$  (D) conditions, Ac4PIM6 under  $T_H1$  (E) or  $T_H2$  (F) conditions and cardioliplin under  $T_H1$  (G) or  $T_H2$  (H) conditions in  $T_H1/T_H2$  differentiation are shown.

to CD4 T cells to enhance the generation of IFN- $\gamma$ -producing cells and inhibit the generation of IL-4-producing cells under  $T_H2$  culture conditions. IL-12 appears to play an important role in the indirect regulation by LAM/LM.

#### Effects of purified LAM and LM in human $T_H1/T_H2$ differentiation cultures

The balance of ManLAM/LM is considered to be important for the protection from mycobacterial infection (34). To further confirm the effects of LAM and LM on the  $T_H1/T_H2$  differentiation, each component was purified from the mixture of LAM/LM and added into the  $T_H1/T_H2$  cultures. Under  $T_H1$  culture conditions, both LAM and LM enhanced the IFN- $\gamma$ -producing  $T_H1$  cells (58.8 versus 67.3 and 65.5%, respectively), although the levels were slightly lower than those of the cultures with LAM/LM mixture (83.0%; Fig. 8, upper panels). Under  $T_H2$  culture conditions, LAM and LM also induced the generation of

IFN- $\gamma$ -producing  $T_H1$  cells (18.1 versus 35.0 and 29.5%, respectively; Fig. 8, lower panels). No obvious inhibition of the generation of IL-4-producing cells was observed in the presence of LAM or LM. These results indicate that both LAM and LM components possess the ability to enhance  $T_H1$  differentiation. In addition, the balance of LAM/LM may also contribute to the effect on  $T_H$  differentiation.

#### Discussion

The present study using an *in vitro*  $T_H1/T_H2$  differentiation culture system with human peripheral blood naive CD4 T cells demonstrated that LAM/LM from *M. bovis* BCG enhanced  $T_H1$  differentiation by two distinct pathways (Fig. 9). LAM/LM acts directly to naive CD4 T cells to enhance  $T_H1$  cell differentiation under  $T_H1$  culture conditions. LAM/LM also acts indirectly via DCs to induce polarization in  $T_H$  differentiation from  $T_H2$  to  $T_H1$  under  $T_H2$  culture conditions.

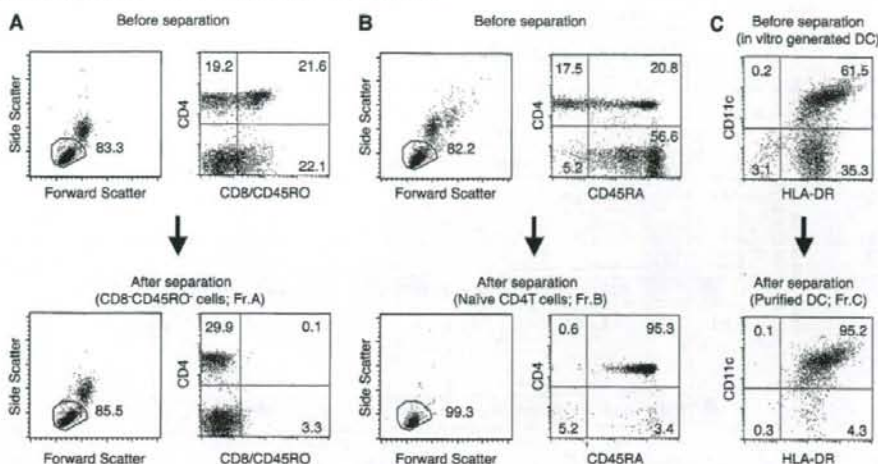


**Fig. 6.** Enrichment of human naive CD4 T cells and DCs. (A) Isolation of naive CD4 (CD8<sup>+</sup>CD45RO<sup>-</sup>) T cells (Fraction A). Human PBMCs were stained with FITC-conjugated anti-CD8 mAb, FITC-conjugated anti-CD45RO mAb and anti-FITC magnetic beads and then sorted the negative fraction using an AutoMACS<sup>®</sup> cell sorter. The percentages of cells in each gate are shown. (B) Isolation of purified CD4 T cells (Fr. B). Naive CD4<sup>+</sup> T cells were isolated from human PBMCs using human naive CD4<sup>+</sup> T cell isolation kit and AutoMACS<sup>®</sup> cell sorter. The purity of CD4<sup>+</sup> cells was 95.3%. (C) Purification of DCs from *in vitro*-generated DCs. *In vitro*-cultured DCs were stained with PE-conjugated anti-CD11c mAb, and the positive fraction of the anti-PE mAb-coupled magnetic beads were purified using an AutoMACS<sup>®</sup> cell sorter. The purity of the DCs was 95.2%.

It is reported in mouse system that TLRs recognize LMs, and TLR2 play important roles in the induction of type-I inflammatory responses (40–42). The signals via TLR2 induced the expression of CD1 and T cell activation (43). Gilleron *et al.* showed that PIM2 and PIM6, which are the anchor motif of LAM/LM, activate primary macrophages to secrete TNF $\alpha$  through TLR2, irrespective of their acylation pattern (44). These results suggest that PIM2 and PIM6 activate APC via TLR2. In the current study, however, PIM2 and PIM6 did not enhance  $T_H1$  differentiation under  $T_H1$  culture conditions, but enhanced  $T_H2$  differentiation in some individuals under  $T_H2$  culture conditions (Fig. 3C). These results suggest that PIM2 and PIM6 may negatively regulate  $T_H1$  generation through the enhanced differentiation of  $T_H2$  under  $T_H2$  conditions. The discrepancies in the response of APC against PIM2 and PIM6 may be due to the difference in the physicochemical properties of micelle sizes or the solvent used between the PIM products of Gilleron *et al.* (44) and ours. The former PIMs are less polar than that of LAM/LM and produce larger micelle particles in the endocytotic process. In any event, it is likely that LAM/LM stimulates DCs via TLR2 and modifies the balance of  $T_H1$ / $T_H2$  differentiation.

To examine the cellular mechanisms underlying the effect of LAM/LM on the  $T_H1$ / $T_H2$  differentiation, the results with a crude naive CD4 T cell fraction and a highly purified naive CD4 T cell fraction after eliminating APCs were compared. Interestingly, the enhanced generation of  $T_H1$  by LAM/LM under  $T_H1$  culture conditions can be seen markedly in the absence of APCs, but the inhibition of  $T_H2$  generation under  $T_H2$  culture conditions is totally dependent on APCs (Fig. 7). Human CD4 T cells express various types of TLRs including TLR2, 5 and 7/8 (45). In another report, human naive CD4

T cells were found to express undetectable levels of TLR2 but the expression was significantly increased after anti-CD3 stimulation (46). The expression of TLRs was examined in our purified CD4 T cells and it was revealed that the purified CD4 T cells express substantial mRNA levels of TLR1, 2, 5, 7, 9 and 10 (Ito, T. and Nakayama, T., unpublished observation). Thus, it is likely that LAM/LM binds directly to one of these TLRs and induces polarization toward  $T_H1$  differentiation. Recently, in a mouse system, stimulation through TLR2 on  $T_H1$  cells was observed to induce IFN- $\gamma$  production and proliferation, and this effect is augmented by IL-2 or IL-12 (47). Thus, it is likely that LAM/LM acts on early activated CD4 T cells and also on developing  $T_H1$  in the culture and resulted in the polarized  $T_H1$  differentiation.

In the cultures under neutral conditions, the cytokine auto-regulatory loops may proceed, and the effects observed under neutral conditions may be more reflective of the *in vivo* effects of LAM/LM. Unfortunately, in human CD4 T cell cultures, the differentiation of naive T cells into  $T_H1$ / $T_H2$  cells was not efficiently observed under neutral conditions, and no obvious effect of LAM/LM was detected (Figs 3 and 7). However, we observed increases in the generation of IFN- $\gamma$ -producing cells when we added DCs to the purified CD4 T cell cultures (Fig. 7). Based on these results, we concluded that even under neutral conditions, LAM/LM has an enhancing effect on the generation of IFN- $\gamma$ -producing  $T_H1$ . We will investigate the effect of LAM/LM in the presence of various kinds of DCs under neutral conditions in the near future.

It is possible that NKT cells play a role in the observed LAM/LM-mediated induction of  $T_H1$  differentiation (48, 49). However, during the process of the magnetic separation of CD8<sup>+</sup>CD45RO<sup>-</sup> cells (naive CD4 T cells, Fr. A in Fig. 6A), all

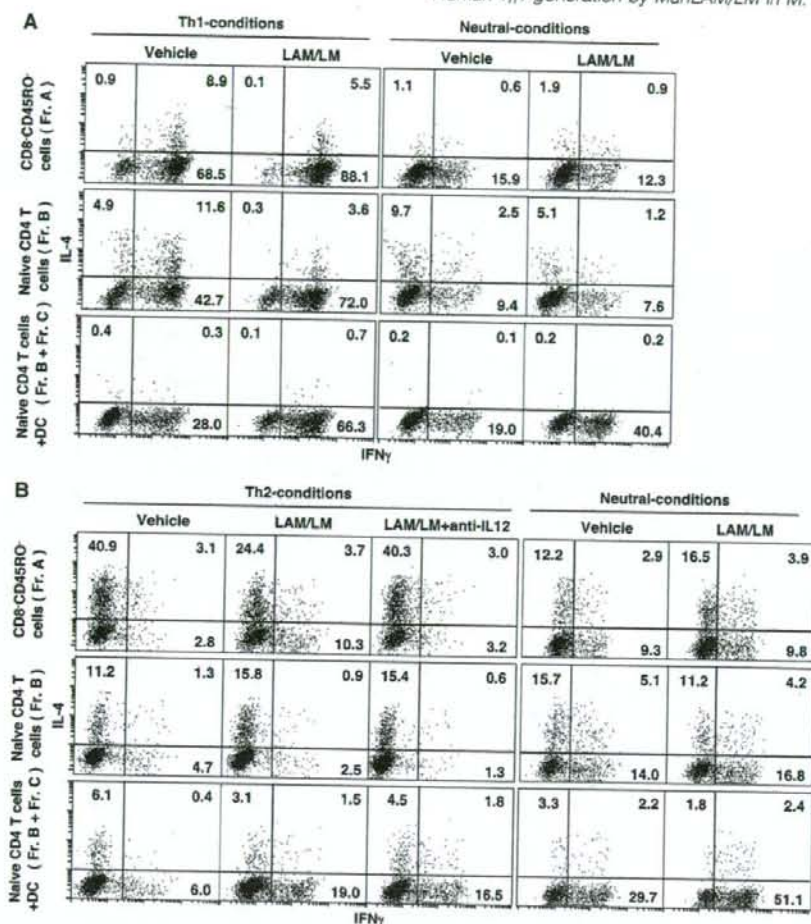


**Fig. 7.** Roles of DCs in the effect of LAM/LM on  $T_H1/T_H2$  differentiation. Naive CD4 T cells (CD8<sup>-</sup>CD45RO<sup>-</sup> cells) (Fr. A), purified CD4 T cells (Fr. B) and DCs (Fr. C) were stimulated with anti-CD3 under  $T_H1$  (panel A, cultured for a week),  $T_H2$  (panel B, cultured for 2 weeks) or neutral culture conditions (panels A and B, cultured for 1 or 2 weeks, respectively). Anti-IL-12 mAb was added at the beginning of  $T_H2$  cultures. Intracellular staining profiles of IFN- $\gamma$ /IL-4 are shown with percentages of cells in each area. Three experiments were performed with similar results.

V $\alpha$ 24 NKT cells appeared to be eliminated and undetectable in our preparing naive CD4 T cells (Ito, T. and Nakayama, T., unpublished observation). Therefore, it is unlikely that V $\alpha$ 24 NKT cells are involved in the LAM/LM-mediated induction of  $T_H1$  differentiation.

There are three types of capping motifs in LAM molecules. One is named ManLAM having a mannosyl cap, and this is isolated from *M. tuberculosis* and *M. bovis* including BCG subspecies and *Mycobacterium kansasii*. Another is PILAM, which has a phosphoinositol cap, and is isolated from *M. smegmatis*. The third one is AraLAM, which has no capping motif, and is isolated from *Mycobacterium chelonae* (44). It is reported that LAM and PILAM but not ManLAM or AraLAM activate macrophages and DCs to secrete IL-12 (26, 50, 51).

On the other hand, LM but not PIM induces apoptosis or activates these cells to secrete IL-12 (25, 52). These results may indicate that ManLAM possesses the ability to inhibit LM-induced apoptosis and IL-12 secretion. In the present study, both LAM and LM components showed the enhancing activity of  $T_H1$  differentiation (Fig. 8). However, we did not detect any inhibiting effects on the generation of IL-4-producing  $T_H2$  (Fig. 8). We think that the inhibition of the generation of IL-4-secreting cells is a secondary effect by the enhancement of the generation of IFN- $\gamma$ -producing cells because the inhibition was neutralized by the addition of anti-IL-12 mAb (Fig. 7). Since the effects of LAM and LM on the generation of IFN- $\gamma$ -producing cells were milder than LAM/LM, we may not be able to detect the inhibition of the

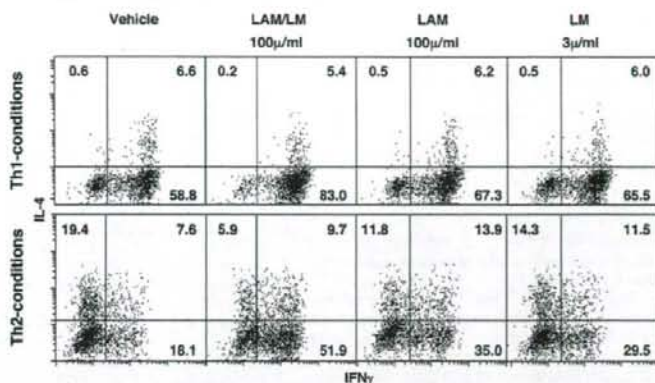


**Fig. 8.** Effects of purified LAM or LM components on human PBMC  $T_H1/T_H2$  differentiation. Naive CD4 T cells from human PBMC were cultured with LAM/LM ( $100 \mu\text{g ml}^{-1}$ ), LAM ( $30$  and  $100 \mu\text{g ml}^{-1}$ ) or LM ( $3$  and  $30 \mu\text{g ml}^{-1}$ ) under  $T_H1/T_H2$  cultured conditions. The intracellular staining profiles of IFN- $\gamma$ /IL-4 are shown with percentages of cells in each area. Three experiments were performed with similar results.

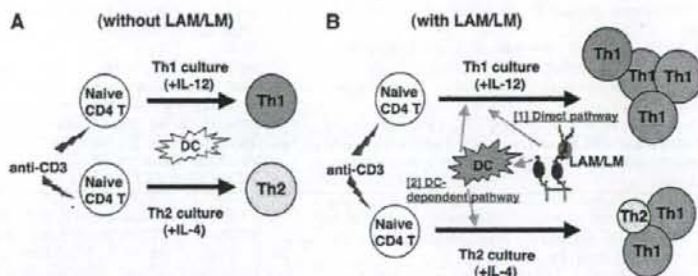


**Fig. 9.** Two distinct regulatory pathways for  $T_H1$  generation induced by LAM/LM in human  $T_H1/T_H2$  cultures. In the presence of LAM/LM, the generation of  $T_H1$  cells was enhanced both under  $T_H1$  culture conditions and  $T_H2$  culture conditions (panel B). Under  $T_H1$  conditions, LAM/LM directly act on CD4 T cells (direct pathway). LAM/LM act on DCs (DC-dependent pathway) and then induce the enhancement of  $T_H1$  differentiation under both  $T_H1$  and  $T_H2$  conditions.

production of IL-4-secreting cells by LAM or LM (Fig. 8). LM appears to induce  $T_H1$  differentiation more prominently in lower doses than LAM (Ito, T., and Nakayama, T., unpublished observation). In addition, high doses of LM did not show the enhancing effect in  $T_H1$  differentiation (Ito, T., and Nakayama, T., unpublished observation). These results may suggest that the balance of LAM/LM is critically important for the induction of  $T_H1$  responses. Further investigations on the effect of the balance of LAM/LM in the human immune system may contribute to the development of new immunotherapeutic approaches for allergic diseases, cancer and infectious diseases.

#### Supplementary data

Supplementary Figure 1 available at *International Immunology Online*.

#### Funding

Ministry of Education, Culture, Sports, Science and Technology (Japan) [Grants-in-Aid: for Scientific Research on Priority Areas #17016010; Scientific Research (B) #17390139,

Scientific Research (C) #18590466, #19590491 and #19591609, Exploratory Research #19659121 and Young Scientists (Start-up) #18890046; Special Coordination Funds for Promoting Science and Technology and Cancer Translational Research Project; Ministry of Health, Labor and Welfare (Japan); The Japan Health Science Foundation; Kanae Foundation; Uehara Memorial Foundation; Mochida Foundation; Yasuda Medical Foundation; Astellas Foundation; Sagawa Foundation.

#### Acknowledgements

We thank Kaoru Sugaya, Hikari Asou and Satoko Norikane for their excellent technical assistance.

#### Abbreviations

APC	antigen presenting cell
BCG	Bacille Calmett-Guérin
CW	cell wall
DC	dendritic cell
LAM	lipoarabinomannan

LM	lipomannan
ManLAM	LAM with mannose caps
PI	phosphatidylinositol
PIM	phosphatidylinositol mannosides
PIM2	phosphatidylinositol dimannoside
PIM6	phosphatidylinositol hexamannoside
TLR2	Toll-like receptor 2
TNF $\alpha$	tumor necrosis factor $\alpha$

## References

- Besra, G. S., Morehouse, C. B., Rittner, C. M., Waechter, C. J. and Brennan, P. J. 1997. Biosynthesis of mycobacterial lipoarabinomannan. *J. Biol. Chem.* 272:18460.
- Nigou, J., Gilleron, M. and Puzo, G. 1999. Lipoarabinomannans: characterization of the multiacylated forms of the phosphatidylinositol anchor by NMR spectroscopy. *Biochem. J.* 337:453.
- Sibley, L. D., Hunter, S. W., Brennan, P. J. and Krahenbuhl, J. L. 1988. Mycobacterial lipoarabinomannan inhibits gamma interferon-mediated activation of macrophages. *Infect. Immun.* 56:1232.
- Sibley, L. D., Adams, L. B. and Krahenbuhl, J. L. 1990. Inhibition of interferon-gamma-mediated activation in mouse macrophages treated with lipoarabinomannan. *Clin. Exp. Immunol.* 80:141.
- Moreno, C., Mehler, A. and Lamb, J. 1988. The inhibitory effects of mycobacterial lipoarabinomannan and polysaccharides upon polyclonal and monoclonal human T cell proliferation. *Clin. Exp. Immunol.* 74:206.
- Chan, J., Fan, X. D., Hunter, S. W., Brennan, P. J. and Bloom, B. R. 1991. Lipoarabinomannan, a possible virulence factor involved in persistence of *Mycobacterium tuberculosis* within macrophages. *Infect. Immun.* 59:1755.
- Schlesinger, L. S., Hull, S. R. and Kaufman, T. M. 1994. Binding of the terminal mannosyl units of lipoarabinomannan from a virulent strain of *Mycobacterium tuberculosis* to human macrophages. *J. Immunol.* 152:4070.
- Apostolou, I., Takahama, Y., Beilant, C. et al. 1999. Murine natural killer T(NKT) cells [correction of natural killer cells] contribute to the granulomatous reaction caused by mycobacterial cell walls. *Proc. Natl Acad. Sci. USA* 96:5141.
- Gilleron, M., Ronet, C., Mempel, M., Monsarrat, B., Gachelin, G. and Puzo, G. 2001. Acylation state of the phosphatidylinositol mannosides from *Mycobacterium bovis* bacillus Calmette Guerin and ability to induce granuloma and recruit natural killer T cells. *J. Biol. Chem.* 276:34896.
- Khoo, K. H., Dell, A., Morris, H. R., Brennan, P. J. and Chatterjee, D. 1995. Structural definition of acylated phosphatidylinositol mannosides from *Mycobacterium tuberculosis*: definition of a common anchor for lipomannan and lipoarabinomannan. *Glycobiology* 5:117.
- Schaeffer, M. L., Khoo, K. H., Besra, G. S. et al. 1999. The *pimB* gene of *Mycobacterium tuberculosis* encodes a mannosyltransferase involved in lipoarabinomannan biosynthesis. *J. Biol. Chem.* 274:31625.
- Kremer, L., Gurucha, S. S., Bifani, P. et al. 2002. Characterization of a putative  $\alpha$ -mannosyltransferase involved in phosphatidylinositol trimannoside biosynthesis in *Mycobacterium tuberculosis*. *Biochem. J.* 363:437.
- Hunter, S. W. and Brennan, P. J. 1990. Evidence for the presence of a phosphatidylinositol anchor on the lipoarabinomannan and lipomannan of *Mycobacterium tuberculosis*. *J. Biol. Chem.* 265:9272.
- Banchereau, J. and Steinman, R. M. 1998. Dendritic cells and the control of immunity. *Nature* 392:245.
- Cella, M., Sallusto, F. and Lanzavecchia, A. 1997. Origin, maturation and antigen presenting function of dendritic cells. *Curr. Opin. Immunol.* 9:10.
- Reis e Sousa, C., Sher, A. and Kaye, P. 1999. The role of dendritic cells in the induction and regulation of immunity to microbial infection. *Curr. Opin. Immunol.* 11:392.
- Demangel, C., Bean, A. G., Martin, E., Feng, C. G., Kamath, A. T. and Britton, W. J. 1999. Protection against aerosol *Mycobacterium tuberculosis* infection using *Mycobacterium bovis* Bacillus Calmette Guerin-infected dendritic cells. *Eur. J. Immunol.* 29:1972.
- Thurnher, M., Ramoner, R., Gastl, G. et al. 1997. Bacillus Calmette-Guérin mycobacteria stimulate human blood dendritic cells. *Int. J. Cancer.* 70:128.
- Tascon, R. E., Soares, C. S., Ragno, S., Stavropoulos, E., Hirst, E. M. and Colston, M. J. 2000. *Mycobacterium tuberculosis*-activated dendritic cells induce protective immunity in mice. *Immunology.* 99:473.
- Cooper, A. M., Dalton, D. K., Stewart, T. A., Griffin, J. P., Russell, D. G. and Orme, I. M. 1993. Disseminated tuberculosis in interferon  $\gamma$  gene-disrupted mice. *J. Exp. Med.* 178:2243.
- Flynn, J. L., Chan, J., Triebold, K. J., Dalton, D. K., Stewart, T. A. and Bloom, B. R. 1993. An essential role for interferon  $\gamma$  in resistance to *Mycobacterium tuberculosis* infection. *J. Exp. Med.* 178:2249.
- Dalton, D. K., Haynes, L., Chu, C. Q., Swain, S. L. and Wittmer, S. 2000. Interferon  $\gamma$  eliminates responding CD4 T cells during mycobacterial infection by inducing apoptosis of activated CD4 T cells. *J. Exp. Med.* 192:117.
- Li, X., McKinstry, K. K., Swain, S. L. and Dalton, D. K. 2007. IFN- $\gamma$  acts directly on activated CD4<sup>+</sup> T cells during mycobacterial infection to promote apoptosis by inducing components of the intracellular apoptosis machinery and by inducing extracellular proapoptotic signals. *J. Immunol.* 179:939.
- Ottenhoff, T. H., Kumararatne, D. and Casanova, J. L. 1998. Novel human immunodeficiencies reveal the essential role of type-I cytokines in immunity to intracellular bacteria. *Immunol. Today.* 19:491.
- Nigou, J., Zelle-Rieser, C., Gilleron, M., Thurnher, M. and Puzo, G. 2001. Mannosylated lipoarabinomannans inhibit IL-12 production by human dendritic cells: evidence for a negative signal delivered through the mannose receptor. *J. Immunol.* 166:7477.
- Geijtenbeek, T. B., Van Vliet, S. J., Koppel, E. A. et al. 2003. Mycobacteria target DC-SIGN to suppress dendritic cell function. *J. Exp. Med.* 197:7.
- Tailleux, L., Maeda, N., Nigou, J., Gicquel, B. and Neyrolles, O. 2003. How is the phagocyte lectin keyboard played? Master class lesson by *Mycobacterium tuberculosis*. *Trends Microbiol.* 11:259.
- Gilleron, M., Himoudi, N., Adam, O. et al. 1997. *Mycobacterium smegmatis* phosphoinositols-glycerol-arabinomannans. Structure and localization of alkali-labile and alkali-stable phosphoinositides. *J. Biol. Chem.* 272:117.
- Adams, L. B., Fukutomi, Y. and Krahenbuhl, J. L. 1993. Regulation of murine macrophage effector functions by lipoarabinomannan from mycobacterial strains with different degrees of virulence. *Infect. Immun.* 61:4173.
- Means, T. K., Lien, E., Yoshimura, A., Wang, S., Golenbock, D. T. and Fenton, M. J. 1999. The CD14 ligand lipoarabinomannan and lipopolysaccharide differ in their requirement for Toll-like receptors. *J. Immunol.* 163:6748.
- Vignal, C., Guerardel, Y., Kremer, L. et al. 2003. Lipomannans, but not lipoarabinomannans, purified from *Mycobacterium chelonae* and *Mycobacterium kansasii* induce TNF- $\alpha$  and IL-8 secretion by a CD14-toll-like receptor 2-dependent mechanism. *J. Immunol.* 171:2014.
- Quesniaux, V. J., Nicolle, D. M., Torres, D. et al. 2004. Toll-like receptor 2 (TLR2)-dependent-positive and TLR2-independent-negative regulation of proinflammatory cytokines by mycobacterial lipomannans. *J. Immunol.* 172:4425.
- Dao, D. N., Kremer, L., Guerardel, Y. et al. 2004. *Mycobacterium tuberculosis* lipomannan induces apoptosis and interleukin-12 production in macrophages. *Infect. Immun.* 72:2067.
- Briken, V., Porcellì, S. A., Besra, G. S. and Kremer, L. 2004. Mycobacterial lipoarabinomannan and related lipoglycans: from biogenesis to modulation of the immune response. *Mol. Microbiol.* 53:391.
- Fujita, Y., Doi, T., Sato, K. and Yano, I. 2005. Diverse humoral immune responses and changes in IgG antibody levels against mycobacterial lipid antigens in active tuberculosis. *Microbiology.* 151:2065.
- Nigou, J., Gilleron, M., Cahuzac, B. et al. 1997. The phosphatidylinositol anchor of the lipoarabinomannans from *Mycobacterium*

- bovis* bacillus Calmette Guerin. Heterogeneity, structure, and role in the regulation of cytokine secretion. *J. Biol. Chem.* 272:23094.
- 37 Motohashi, S., Kobayashi, S., Ito, T. *et al.* 2002. Preserved IFN- $\alpha$  production of circulating V $\alpha$ 24 NKT cells in primary lung cancer patients. *Int. J. Cancer.* 102:159.
- 38 Ishikawa, E., Motohashi, S., Ishikawa, A. *et al.* 2005. Dendritic cell maturation by CD11c- T cells and V $\alpha$ 24\* natural killer T-cell activation by  $\alpha$ -galactosylceramide. *Int. J. Cancer.* 117:265.
- 39 Kaneko, T., Hosokawa, H., Yamashita, M. *et al.* 2007. Chromatin remodeling at the Th2 cytokine gene loci in human type 2 helper T cells. *Mol. Immunol.* 44:2249.
- 40 Fricke, I., Mitchell, D., Mittelstadt, J. *et al.* 2006. Mycobacteria induce IFN- $\gamma$  production in human dendritic cells via triggering of TLR2. *J. Immunol.* 176:5173.
- 41 Gilleron, M., Nigou, J., Nicolle, D., Quesniaux, V. and Puzo, G. 2006. The acylation state of mycobacterial lipomannans modulates innate immunity response through toll-like receptor 2. *Chem. Biol.* 13:39.
- 42 Dabbagh, K. and Lewis, D. B. 2003. Toll-like receptors and T-helper-1/T-helper-2 responses. *Curr. Opin. Infect. Dis.* 16:199.
- 43 Foura-Mir, C., Wang, L., Cheng, T. Y. *et al.* 2005. *Mycobacterium tuberculosis* regulates CD1 antigen presentation pathways through TLR-2. *J. Immunol.* 175:1758.
- 44 Nigou, J., Gilleron, M. and Puzo, G. 2003. Lipoarabinomannans: from structure to biosynthesis. *Biochimie.* 85:153.
- 45 Kabelitz, D. 2007. Expression and function of Toll-like receptors in T lymphocytes. *Curr. Opin. Immunol.* 19:39.
- 46 Xu, D., Komai-Koma, M. and Liew, F. Y. 2005. Expression and function of Toll-like receptor on T cells. *Cell. Immunol.* 233:85.
- 47 Imanishi, T., Hara, H., Suzuki, S., Suzuki, N., Akira, S. and Saito, T. 2007. Cutting edge: tLR2 directly triggers Th1 effector functions. *J. Immunol.* 178:6715.
- 48 Emoto, M., Emoto, Y., Buchwalow, I. B. and Kaufmann, S. H. 1999. Induction of IFN- $\gamma$ -producing CD4\* natural killer T cells by *Mycobacterium bovis* bacillus Calmette Guerin. *Eur. J. Immunol.* 29:650.
- 49 Dieli, F., Taniguchi, M., Kronenberg, M. *et al.* 2003. An anti-inflammatory role for V $\alpha$ 14 NK T cells in *Mycobacterium bovis* bacillus Calmette-Guérin-infected mice. *J. Immunol.* 171:1961.
- 50 Rojas, M., Garcia, L. F., Nigou, J., Puzo, G. and Olivier, M. 2000. Mannosylated lipoarabinomannan antagonizes *Mycobacterium tuberculosis*-induced macrophage apoptosis by altering Ca<sup>2+</sup>-dependent cell signaling. *J. Infect. Dis.* 182:240.
- 51 Yoshida, A. and Koide, Y. 1997. Arabinfuranosyl-terminated and mannosylated lipoarabinomannans from *Mycobacterium tuberculosis* induce different levels of interleukin-12 expression in murine macrophages. *Infect. Immun.* 65:1953.
- 52 Nigou, J., Gilleron, M., Rojas, M., Garcia, L. F., Thurnher, M. and Puzo, G. 2002. Mycobacterial lipoarabinomannans: modulators of dendritic cell function and the apoptotic response. *Microbes Infect.* 4:945.



# Homo-oligomerization Is Essential for Toll/Interleukin-1 Receptor Domain-containing Adaptor Molecule-1-mediated NF- $\kappa$ B and Interferon Regulatory Factor-3 Activation\*

Received for publication, February 7, 2008, and in revised form, April 22, 2008. Published, JBC Papers in Press, May 1, 2008, DOI 10.1074/jbc.M801013200

Kenji Funami<sup>1,2</sup>, Miwa Sasai<sup>1,3</sup>, Hiroyuki Oshiumi, Tsukasa Seya, and Misako Matsumoto<sup>4</sup>

From the Department of Microbiology and Immunology, Hokkaido University Graduate School of Medicine, Kita-15, Nishi-7, Kita-ku, Sapporo 060-8638, Japan

Toll-IL-1 receptor (TIR) domain-containing adaptor molecule-1 (TICAM-1, also named TIR domain-containing adaptor-inducing interferon ( $\text{IFN}$ )- $\beta$  or TRIF)) is a signaling adaptor of Toll-like receptor (TLR) 3/4 that activates the transcription factors, interferon regulatory factor-3 (IRF-3) and NF- $\kappa$ B leading to inducing  $\text{IFN}$ - $\beta$  production. The mechanisms by which TICAM-1 is activated by TLR3/4 to serve as a signaling platform are unknown. In this study, we show that homo-oligomerization of TICAM-1 is critical for TICAM-1-mediated activation of NF- $\kappa$ B and IRF-3. Both TIR and C-terminal domain of TICAM-1 mediated TICAM-1 oligomerization. Pro<sup>434</sup> located in the TIR domain and the C-terminal region, with the exception of the RIP homotypic-interacting motif, were determinants of TICAM-1 oligomerization. Mutation of TIR domain (P434H) or deletion of C-terminal domain greatly reduced TICAM-1-mediated NF- $\kappa$ B and  $\text{IFN}$ - $\beta$  promoter activation. TICAM-1 oligomerization at either the TIR domain or the C-terminal region resulted in recruitment of tumor necrosis factor receptor-associated factor 3, a downstream signaling molecule essential for TICAM-1-mediated IRF-3 activation, but not recruitment of the IRF-3 kinase complex, NF- $\kappa$ B-activating kinase-associated protein 1 and TANK-binding kinase 1. In addition, RIP homotypic-interacting motif mutant, which possesses two oligomerization motifs but not the RIP1 binding motif, also failed to recruit NF- $\kappa$ B-activating kinase-associated protein 1 and TANK-binding kinase 1. Thus, full activation and formation of TICAM-1 signalosomes requires oligomerization induced at two different sites and RIP1 binding.

The innate immune system senses bacterial and viral infections using Toll-like receptors (TLRs)<sup>5</sup> and cytoplasmic

pattern-recognition receptors. Endosomal TLRs and cytoplasmic DEAD/H box RNA helicases, retinoic acid-inducible gene-1 (RIG-I) and melanoma differentiation-associated gene 5 (MDA5), play key roles in anti-viral immunity by inducing transcription of type I interferon ( $\text{IFN}$ ) and  $\text{IFN}$ -regulatory genes (1, 2).

Among these receptors, TLR3 has distinct properties that allow recognition of extracellular virus-derived double-stranded RNA (dsRNA) and induction of type I  $\text{IFN}$ /cytokine production and dendritic cell maturation that results in activation of natural killer cells and cytotoxic T lymphocytes (3–6). TLR3 signaling is mediated via an adaptor molecule, Toll-IL-1 receptor (TIR) domain-containing adaptor molecule-1 (TICAM-1, also named TIR domain-containing adaptor inducing  $\text{IFN}$ - $\beta$  (TRIF)), which activates the transcription factors interferon regulatory factor-3 (IRF-3), NF- $\kappa$ B, and AP-1 (7, 8). TICAM-1 consists of a proline-rich N-terminal region, a TIR domain, and a C-terminal region. The TIR domain of TICAM-1 is essential for binding to the TIR domain of TLR3 as well as to the TLR4 adaptor molecule, TICAM-2 (also called TRIF-related adaptor molecule) (9, 10). The N-terminal region is crucial for TICAM-1-mediated IRF-3 activation via recruitment of IRF-3-activating kinases, TANK-binding kinase 1 (TBK1) and inhibitor of nuclear factor  $\kappa$ B kinase  $\epsilon$  (IKK $\epsilon$ , also called IKK $\iota$ ) (7, 11–13). The C-terminal region is involved in NF- $\kappa$ B activation and induction of apoptosis via binding of the receptor interacting protein (RIP) 1 to the RIP homotypic-interacting motif (RHIM) domain (14, 15). The NF- $\kappa$ B-activating kinase-associated protein 1 (NAP1) and tumor necrosis factor receptor-associated factor 3 (TRAF3) are found downstream of TICAM-1 and are involved in the TICAM-1-mediated activation of IRF-3 (16–18).

NAP1 and TRAF3 are also involved in RIG-I/MDA5-mediated production of  $\text{IFN}$ - $\beta$  through interactions with the adaptor molecule,  $\text{IFN}$ - $\beta$  promoter stimulator 1 (also called MAVS, Cardif, or VISA) (19–24).  $\text{IFN}$ - $\beta$  promoter stimulator 1 local-

\* This work was supported by Core Research for Evolutional Science and Technology, Japan Science and Technology Corporation, and by Grants-in-Aid from the Ministry of Education, Science, and Culture (Specified Project for Advanced Research) and the hepatitis C virus project of the National Institutes of Health of Japan, and by the Uehara Memorial Foundation, Mitsubishi Foundation, Takeda Foundation, and NorthTec Foundation. The costs of publication of this article were defrayed in part by the payment of page charges. This article must therefore be hereby marked "advertisement" in accordance with 18 U.S.C. Section 1734 solely to indicate this fact.

<sup>1</sup> Both authors contributed equally to this work.

<sup>2</sup> Center for Integrated Medical Research, Keio University, Tokyo 160-8582, Japan.

<sup>3</sup> Dept. of Immunobiology, Yale University School of Medicine, New Haven, CT 06510.

<sup>4</sup> To whom correspondence should be addressed. Tel.: 81-11-706-6056; Fax: 81-11-706-7866; E-mail: matumoto@pop.med.hokudai.ac.jp.

<sup>5</sup> The abbreviations used are: TLR, Toll-like receptor; CARD, caspase recruitment domain; DAPI, 4',6-diamidino-2'-phenylindole; dsRNA, double-

stranded RNA; HA, hemagglutinin;  $\text{IFN}$ - $\beta$ , interferon- $\beta$ ; IRF,  $\text{IFN}$  regulatory factor; MDA5, melanoma differentiation-associated gene 5; NAP1, NF- $\kappa$ B-activating kinase-associated protein 1; RHIM, RIP homotypic interacting motif; RIG-I, retinoic acid-inducible gene 1; RIP1, receptor-interacting protein 1; TBK1, TANK-binding kinase 1; TICAM-1, TIR-containing adaptor molecule-1; TIR, Toll-IL-1 receptor; TRAF, tumor necrosis factor receptor-associated factor; TRIF, TIR domain-containing adaptor-inducing  $\text{IFN}$ - $\beta$ ; Ab, antibody; mAb, monoclonal antibody; pAb, polyclonal antibody; z, benzyl-oxycarbonyl; fmk, fluoromethyl ketone; aa, amino acid(s); PBS, phosphate-buffered saline.

## Homo-oligomerization of TICAM-1

izes to the mitochondrial membrane where it is activated by RIG-I/MDA5 through caspase recruitment domain (CARD)-CARD interactions (20). Although TLR- and RIG-I/MDA5-mediated signaling is transmitted via interaction of unique domain structures, TIR and CARD, respectively, the detailed mechanisms of signal transduction regulated by these domains as well as the spatiotemporal regulation of signaling have not been studied.

TICAM-1 localizes diffusely in the cytosol of resting cells. Once TLR3 is activated by dsRNA, TICAM-1 transiently colocalizes with TLR3, then dissociates from the receptor and forms speckle-like structures with RIP1 and NAP1 (25). In addition, overexpressed TICAM-1 strongly activates the IFN- $\beta$  promoter in a TLR3-independent manner. The mechanisms by which TICAM-1 is activated by receptor ligation or spontaneously following overexpression are unknown. In this study, we constructed various TICAM-1 mutants and used a yeast two-hybrid system and immunoprecipitation studies to identify the critical regions involved in TICAM-1 oligomerization. We show that full activation and formation of TICAM-1 signalosomes require oligomerization induced at two different sites and RIP1 binding. Furthermore, we demonstrate that, during TLR3/4-TICAM-1-signaling, the conserved proline residue within the BB loop of the upstream TIR domain determines the interaction with the downstream TIR domain, which in turn leads to signal transduction.

### EXPERIMENTAL PROCEDURES

**Cell Culture and Reagents**—HEK293 cells and HEK293FT cells were maintained in Dulbecco's Modified Eagle's medium (Invitrogen) supplemented with 10% heat-inactivated fetal calf serum (Invitrogen) and antibiotics. HeLa cells were maintained in MEM (Nissui, Tokyo, Japan) supplemented with 10% heat-inactivated fetal calf serum. Anti-FLAG M2 mAb, anti-HA pAb, 4',6'-diamidino-2'-phenylindole dihydrochloride (DAPI) and z-VAD-fmk were purchased from Sigma-Aldrich. Alexa Fluor<sup>®</sup>-conjugated secondary antibodies were from Invitrogen. Anti-Myc mAb was from Neomarkers (Lab Vision Corp., Fremont, CA).

**Plasmids**—Complementary DNAs for human TICAM-1, RIP1, and TRAF3 were cloned in our laboratory by reverse transcription-PCR and were ligated into the cloning site of the expression vectors, pEF-BOS and p3xFLAG-CMV-14 (C-terminal 3xFLAG tag). The HA tag was inserted into the C-terminal of each pEF-BOS expression vector for the TICAM-1 mutant. The pCDNA3.1/NAP1-Myc and pCDNA3.1/TBK1-FLAG expression vectors were kindly provided by Dr. M. Nakanishi (Nagoya City University, Nagoya, Japan). Point mutations in the TIR domain (P434H, where Pro<sup>434</sup> was replaced with His) and RHIM domain (<sup>687</sup>VQLG<sup>690</sup>) were replaced with four Ala) were generated by site-directed mutagenesis. The truncated TICAM-1 mutant (N+TIR, 1–566 aa) was generated by PCR using specific primers.

**Yeast Two-hybrid Assay**—The yeast two-hybrid assay was performed as described previously (7). The yeast AH109 strain (Clontech, Palo Alto, CA) was transformed using bait (pGBKT7) and prey (pGADT7) plasmids. The transformants were streaked onto plates and incubated for 3–5 days. BD and

AD in the figures represent the bait and prey plasmid, respectively. The various BD- and AD-TICAM-1 mutants were constructed by inserting each cDNA fragment into the pGBKT7 (bait) or pGADT7 (prey) plasmids (Clontech). BD-TLR3-TIR and AD-TLR3-TIR were constructed by inserting the cDNA fragment encoding the TIR domain of TLR3 into the pGBKT7 or pGADT7 plasmids. BD-TICAM-2 and AD-TICAM-2 were constructed by inserting the full-length TICAM-2 cDNA into the pGBKT7 or pGADT7 plasmids. SD-WLH is a yeast synthetic dextrose medium that lacks Trp, Leu, and His amino acids. SD-WLHA lacks adenine in addition to Trp, Leu, and His.

**Confocal Microscopy**—HeLa cells ( $1.0 \times 10^5$  cells/well) were plated onto micro cover glasses (Matsunami, Tokyo, Japan) in a 24-well plate. The following day, cells were transfected with the indicated plasmids using FuGENE HD (Roche Diagnostics). The total amount of DNA (0.5  $\mu$ g/well) was kept constant by adding empty vector. In the cells transfected with wild-type TICAM-1 and the P434H mutant, z-VAD-fmk (20  $\mu$ M) was added to the cells before transfection to inhibit apoptosis. Twenty-four hours after transfection, cells were fixed using 10% formaldehyde in PBS and permeabilized with PBS containing 0.2% Triton X-100 for 15 min. Fixed cells were blocked in PBS containing 1% bovine serum albumin and labeled with the indicated primary Abs (5  $\mu$ g/ml) for 60 min at room temperature. Alexa-conjugated secondary Abs (1:400) were used to visualize staining of the primary Abs. Nuclei were stained with DAPI (2  $\mu$ g/ml) in PBS for 10 min before mounting onto glass slides using PBS containing 2.3% 1,4-diazabicyclo[2.2.2]octane and 50% glycerol. Cells were visualized at a magnification of  $\times 63$  with an LSM510 META microscope (Zeiss, Jena, Germany).

**Reporter Gene Assay**—HEK293 cells ( $4 \times 10^4$  cells/well) cultured in 96-well plates were transfected with the expression vectors for wild-type TICAM-1, TICAM-1 mutants, or empty vector together with the reporter plasmid (30 ng/well) and an internal control vector, pRL-TK (Promega, Madison, WI) (1 ng/well) using the calcium phosphate method as described previously (26). The p-125 luc reporter contained the human IFN- $\beta$  promoter region (–125 to +19) was provided by Dr. T. Taniguchi (University of Tokyo, Tokyo, Japan). The reporter plasmid containing the ELAM-1 promoter was previously constructed in our laboratory (27). The total amount of DNA (200 ng/well) was kept constant by adding empty vector. After 24 h, cells were lysed in lysis buffer (Promega), and the Firefly and Renilla luciferase activities were determined using a dual-luciferase reporter assay kit (Promega). The Firefly luciferase activity was normalized by Renilla luciferase activity and is expressed as the fold stimulation relative to the activity in vector-transfected cells.

**Immunoprecipitation and Immunoblotting**—HEK293FT cells ( $5 \times 10^5$  cells/well) cultured in 6-well plates were transfected with the indicated plasmids using the calcium phosphate method. For the wild-type TICAM-1 and the TICAM-1 P434H mutant, z-VAD-fmk (20  $\mu$ M) was added to the cells before transfection to inhibit apoptosis. The total amount of DNA (4.0  $\mu$ g/well) was kept constant by adding empty vector. After 24 h, cells were lysed in lysis buffer (20 mM Tris-HCl (pH 7.5) con-

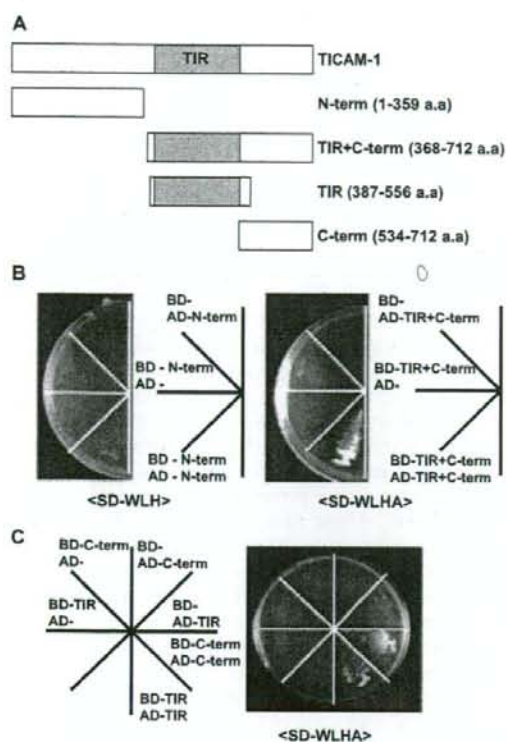


**FIGURE 1. The homodimerization motifs of TICAM-1 are located in both the TIR domain and C-terminal region.** *A*, construction of TICAM-1 mutants for the yeast two-hybrid assay. Each truncated TICAM-1 construct, N-term (1–359 aa), TIR+C-term (368–712 aa), TIR (387–556 aa), or C-term (534–712 aa), was inserted into the pGBKT7 (bait) and the pGADT7 (prey) vectors. The shaded box represents the TIR domain of TICAM-1 (394–533 aa). *B* and *C*, homodimerization of the TICAM-1 mutants in yeast. The TICAM-1 mutant containing the N-terminal region (N-term) failed to homodimerize (*B*, left panel), whereas the TICAM-1 mutant containing the TIR domain and C-terminal region (TIR+C-term) was homodimerized in yeast (*B*, right panel). The TICAM-1 mutants containing only the TIR domain or C-terminal region were homodimerized in the WLHA plate (*C*). *BD* and *AD* represent the bait and prey plasmids, respectively. *SD-WLH* reflects a weak interaction; *SD-WLHA* reflects a strong interaction.

taining 150 mM NaCl, 1% Nonidet P-40, 10 mM EDTA, 25 mM iodoacetamide, 2 mM phenylmethylsulfonyl fluoride, and a protease inhibitor mixture (Roche Applied Science)). Lysates were clarified by centrifugation, pre-cleared with Protein G-Sepharose (GE Healthcare, Buckinghamshire, UK), and incubated with 0.5–2.5  $\mu$ g of Abs. The immunocomplexes were recovered by incubation with Protein G-Sepharose, washed three times with lysis buffer, and resuspended in denaturing buffer. Samples were analyzed by SDS-PAGE (7.5–10%) under reducing conditions followed by immunoblotting with anti-tag Abs.

## RESULTS

**TICAM-1 Homodimerizes via the TIR Domain and C-terminal Region in Yeast**—Upon dsRNA stimulation, TICAM-1 transiently associates with TLR3 before forming a speckle-like structure with downstream signaling molecules (25). The topological dynamics of TICAM-1 secondary to activation by

## Homo-oligomerization of TICAM-1

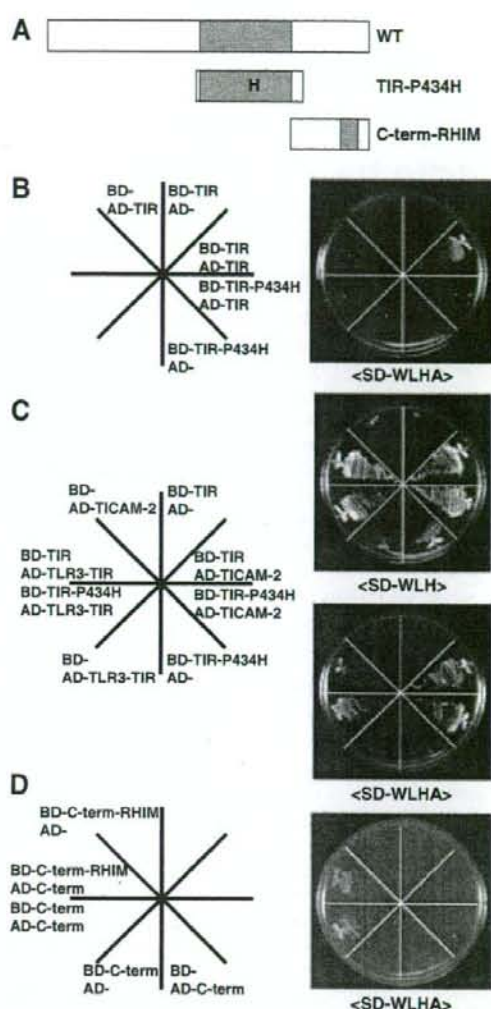


**FIGURE 2. Proline 434 in the TIR domain is critical for homodimerization of TICAM-1 but not for association with TLR3 or TICAM-2.** *A*, construction of TICAM-1 mutants for the yeast two-hybrid assay. The constructs of the TICAM-1 mutant, TIR-P434H (387–556 aa, Pro<sup>434</sup> in the TIR domain is replaced by His) and C-term-RHIM (534–712 aa, 567VQLG<sup>690</sup> within the RHIM domain are replaced with four Ala) were inserted into the pGBKT7 (bait) and the pGADT7 (prey) vectors. *B* and *C*, interactions between the TICAM-1 mutant (TIR-P434H) and wild-type TICAM-1-TIR (TIR), TLR3-TIR, or TICAM-2 in the yeast two-hybrid system. No association was detected between the mutated TIR (TIR-P434H) and wild-type TICAM-1-TIR (*B*), whereas strong association was observed between the TIR-P434H mutant and the TIR of TLR3 (755–904 aa) or TICAM-2 (*C*). *D*, interaction between the C-terminal of TICAM-1 with its RHIM mutant. Association between the RHIM mutant and wild-type C-terminal of TICAM-1 was observed. *BD* and *AD* represent the bait and prey plasmids, respectively.

dsRNA-TLR3 remains unknown, although currently accepted view is that the interaction between TLR3-TIR and TICAM-1-TIR is important for clustering the adaptor molecules around the receptor. Furthermore, overexpressed TICAM-1 forms speckle-like signalosomes in a TLR3-independent manner (25). To examine TICAM-1 oligomerization, we generated several

## Homo-oligomerization of TICAM-1

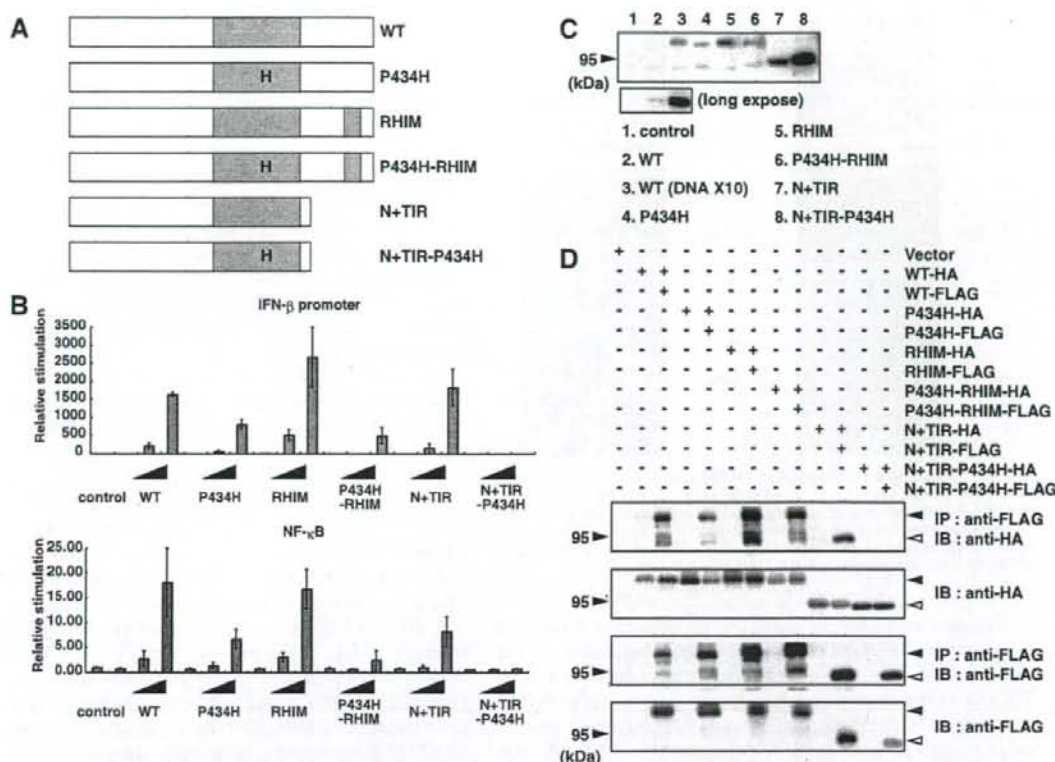


**FIGURE 3. Pro<sup>434</sup> in the TIR domain and the C-terminal RHIM domain are required for full activation of TICAM-1.** *A*, constructs of various TICAM-1 mutants were used. The mutant P434H construct contains a mutated TIR domain in which Pro<sup>434</sup> is substituted with His. The mutant RHIM construct contains a mutated RHIM domain (287VQLG<sup>690</sup> are replaced with four Ala). The mutant P434H-RHIM construct has two mutated sites, Pro<sup>434</sup> and RHIM. The mutant N+TIR (1–566 aa) contains the N-terminal region and the TIR domain and the mutant N+(TIR-P434H) contains the N-terminal region with the mutated TIR-P434H domain. *B*, Pro<sup>434</sup> in the TIR domain and the RHIM domain play an important role in TICAM-1-mediated NF- $\kappa$ B and IFN- $\beta$  promoter activation. HEK293 cells in 96-well plates were transfected with the indicated expression plasmids (0.2, 2.0, and 20.0 ng) together with the IFN- $\beta$  promoter reporter (upper panel, 100 ng) or NF- $\kappa$ B reporter plasmids (lower panel, 100 ng), and pRL-TK (1.0 ng). Twenty-four hours after transfection, the luciferase reporter activities were measured. The average activities from three independent assays are shown as relative stimulation. *C*, HEK293 cells in 24-well plates were transfected with expression plasmids for HA-tagged wild-type TICAM-1 (20 and 200 ng) or each TICAM-1 mutant (20 ng) in the presence of an apoptosis inhibitor. Protein expression levels were determined by immunoblotting using anti-HA pAb. The protein levels of the TICAM-1 mutants are significantly higher than that of wild-type TICAM-1 using the same concentration of DNA plasmid. Lower panel, long exposed membrane. *D*, the homodimerizing ability of the TICAM-1 mutants was assessed using a co-immunoprecipitation assay. HEK293 cells were transfected with the indicated plasmids for HA- or FLAG-tagged TICAM-1 mutants, and cell lysates were immunoprecipitated with anti-FLAG mAb. Immunoprecipitants were resolved on SDS-PAGE under reducing conditions followed by immunoblotting with anti-HA pAb or anti-FLAG mAb. The protein expression in the total cell lysates was analyzed by immunoblotting with anti-HA pAb or anti-FLAG mAb (IB). Only the N+(TIR-P434H) mutant did not homodimerize (upper panel). Closed arrowheads indicate full-length TICAM-1, and open arrowheads indicate the truncated form of TICAM-1 (N+TIR).

truncated TICAM-1 constructs and assayed their homodimerization activities using the yeast two-hybrid system (Fig. 1A). The construct containing the TIR domain and C-terminal region of TICAM-1 induced homodimerization, whereas the construct containing the N-terminal region alone did not (Fig. 1B). Of the constructs that had been truncated further, only the TIR domain or C-terminal region was homodimerized in the yeast system (Fig. 1C) suggesting that TICAM-1 oligomerization is mediated through the TIR domain and C-terminal region.

**TICAM-1 Dimerization Requires the Pro<sup>434</sup> Residue in the TIR Domain and the C-terminal Region with the Exception of the RHIM Domain**—We have previously reported that the TIR domain TIR-P434H mutant acts as a dominant-negative form

during TLR3-mediated signaling (7). In the yeast two-hybrid system, TIR-P434H failed to interact with the TIR domain of TICAM-1 but bound tightly to the tail of TLR3 or TICAM-2 (Figs. 2, A–C). These findings suggest that Pro<sup>434</sup> is critical for the TICAM-1 signaling that mediates TICAM-1 dimerization via the TIR domain. To further identify residues required for mediating TICAM-1 dimerization through the C-terminal region, we generated a TICAM-1 construct consisting of the C-terminal region with a mutated-RHIM domain (Fig. 2A). The RHIM domain is essential for TICAM-1-mediated NF- $\kappa$ B activation and induction of apoptosis via binding of RIP1 (14, 15). Mutation of the RHIM motif did not affect the dimerization of the C-terminal region (Fig. 2D) suggesting that the RHIM motif is dispensable for TICAM-1 dimerization via the C-terminal region.